Neuroscience

# Noradrenaline release from the locus coeruleus shapes stress-induced hippocampal gene expression

**Reviewed Preprint**

Revised by authors after peer review.

About eLife's process

**Reviewed preprint version 2**
February 16, 2024 (this version)

**Reviewed preprint version 1**
August 1, 2023

**Sent for peer review**
April 24, 2023

**Posted to preprint server**
February 2, 2023

**Mattia Privitera, Lukas M. von Ziegler, Amalia Floriou-Servou, Sian N. Duss, Runzhong Zhang, Rebecca Waag, Sebastian Leimbacher, Oliver Sturman, Fabienne K. Roessler, Annelies Heylen, Yannick Vermeiren, Debby Van Dam, Peter P. De Deyn, Pierre-Luc Germain, Johannes Bohacek**

Laboratory of Molecular and Behavioral Neuroscience, Institute for Neuroscience, Department of Health Sciences and Technology, ETH Zurich, Switzerland • Neuroscience Center Zurich, ETH Zurich and University of Zurich, Switzerland • Laboratory of Neurochemistry and Behavior, Experimental Neurobiology Unit, Department of Biomedical Sciences, University of Antwerp, Wilrijk (Antwerp), Belgium • Division of Human Nutrition and Health, Chair Group of Nutritional Biology, Wageningen University & Research (WUR), Wageningen, Netherlands • Department of Neurology and Alzheimer Center, University of Groningen and University Medical Center Groningen (UMCG), Groningen, Netherlands • Department of Neurology, Memory Clinic of Hospital Network Antwerp (ZNA) Middelheim and Hoge Beuken, Antwerp, Belgium • Computational Neurogenomics, Institute for Neuroscience, Department of Health Sciences and Technology, ETH Zürich, Zurich, Switzerland • Laboratory of Statistical Bioinformatics, University of Zürich, Switzerland



## Abstract

Exposure to an acute stressor triggers a complex cascade of neurochemical events in the brain. However, deciphering their individual impact on stress-induced molecular changes remains a major challenge. Here we combine RNA-sequencing with selective pharmacological, chemogenetic and optogenetic manipulations to isolate the contribution of the locus coeruleus - noradrenaline (LC-NA) system to the acute stress response. We reveal that NA-release during stress exposure regulates a large and reproducible set of genes in the dorsal and ventral hippocampus via β-adrenergic receptors. For a smaller subset of these genes, we show that NA release triggered by LC stimulation is sufficient to mimic the stress-induced transcriptional response. We observe these effects in both sexes, and independent of the pattern and frequency of LC activation. Using a retrograde optogenetic approach, we demonstrate that hippocampus-projecting LC neurons directly regulate hippocampal gene expression. Overall, a highly selective set of astrocyte-enriched genes emerges as key targets of LC-NA activation, most prominently several subunits of protein phosphatase 1 (*Ppp1r3c*, *Ppp1r3d*, *Ppp1r3g*) and type II iodothyronine deiodinase (*Dio2*). These results highlight the importance of astrocytic energy metabolism and thyroid hormone signaling in LC-mediated hippocampal function and offer new molecular targets for understanding how NA impacts brain function in health and disease.

**eLife assessment**

This **important** paper uses a multifaceted approach to implicate the locus coeruleus-noradrenaline system in the stress-induced transcriptional changes of dorsal and ventral hippocampus. It provides an inventory of dorsal and ventral hippocampal gene expression upregulated by activation of LC-NA system, which can be used as starting point for more functional studies related to the effects of stress-induced physiological and pathological changes. The results **convincingly** support the conclusions. This paper will be of interest to those interested in stress neurobiology, hippocampal, and/or noradrenaline function.

# Introduction

When an organism faces an acutely stressful situation, a set of evolutionarily conserved mechanisms are triggered to re-route all available resources to body functions that enhance performance and increase the chance of survival (Floriou-Servou et al. 2021; Joëls and Baram 2009). In the brain, stress exposure immediately activates the locus coeruleus-noradrenaline (LC-NA) system. Although the LC is a heterogeneous structure with modular organization, it appears that in stressful situations, broad activation of the LC - and subsequent widespread NA release throughout the brain - serves as a broadcast signal to orchestrate re-routing of computational resources to meet situational demands (Likhtik and Johansen 2019; Poe et al. 2020). On the network level, for example, NA release from the LC is sufficient to trigger a rapid reconfiguration of large-scale networks that shift processing capacity towards salience processing (Zerbi et al. 2019; Oyarzabal et al. 2022). On a circuit level, forebrain regions seem to be particularly important targets of the LC-NA system to influence cognitive processes and ultimately behavior. This involves the engagement of anxiety and memory circuits including the amygdala, hippocampus and prefrontal cortex, which leads to an increase in avoidance behavior (McCall et al. 2015, 2017; Hirschberg et al. 2017; Zerbi et al. 2019) and supports memory formation of salient events (Uematsu, Tan, and Johansen 2015; Hansen 2017; Sara 2015; Schwabe et al. 2022).

While the insights into network and circuit dynamics of the LC have been galvanized by recent advances in circuit neuroscience tools, our understanding of the molecular impact of NA release has remained largely unexplored. However, we know that the stress response triggers multifaceted molecular cascades that profoundly change brain function and behavior in response to stressful events (Floriou-Servou et al. 2021; Joëls and Baram 2009). These molecular changes are mediated by a large number of neurotransmitters, neuropeptides and hormones, which operate on different time scales, to allow rapid activation, sustained activity and successful termination of the stress response. Many of the rapid molecular changes induced by stress exposure seem to be driven by NA. For example, several of the genes that are induced by an acute stress challenge can be blocked by β-adrenergic receptor antagonists (Roszkowski et al. 2016). However, a similar analysis on the genome-wide level has not been conducted. Further, it remains unknown whether NA release alone is sufficient to trigger transcriptomic changes in the first place. Here, we profile the molecular fingerprint of stress-induced NA release by combining pharmacologic, chemogenetic and optogenetic manipulation of the LC-NA system with genome-wide transcriptomic analyses. We focus on the hippocampus, as it receives its sole NA supply from the LC (Loy et al. 1980; Robertson et al. 2013; Oleskevich, Descarries, and Lacaille 1989), and because the molecular response to acute stress has been characterized in great detail in this region (von Ziegler et al. 2022; Mifsud et al. 2021; Floriou-Servou et al. 2018). As the dorsal

hippocampus (dHC) and ventral hippocampus (vHC) are involved in different circuits (Strange et al. 2014) and are transcriptionally very distinct (Cembrowski et al. 2016; Floriou-Servou et al. 2018), we analyze these regions separately.

## Results

A recent multi-omic characterization of the acute stress response in the mouse hippocampus revealed that stress-induced transcriptional changes peak between 45-90 min after stress exposure, before gradually returning to baseline (von Ziegler et al. 2022). To determine how NA might contribute to these effects, we first measured the dynamics of NA turnover in response to a cold swim stress exposure in the brain. Using ultra-high performance liquid chromatography (uHPLC), we determined concentrations of NA and its main metabolite 3-Methoxy-4-hydroxyphenylglycol (MHPG) at various time points over 3 hours after swim stress exposure in the cortex (**Fig. 1a**). NA turnover (as measured by the MHPG/NA ratio) peaked at 45 min and returned to baseline within 90 min after stress onset (**Fig. 1b**). Therefore, we chose the 45 min time point to assess the contribution of NA signaling to stress-induced transcriptomic changes. To this end, we blocked adrenergic receptors using either the α1-adrenergic receptor antagonist prazosin, or the β- adrenergic receptor antagonist propranolol prior to stress exposure (**Fig. 1c**). In line with our previous work (von Ziegler et al. 2022; Floriou-Servou et al. 2018; Roszkowski et al. 2016), acute swim stress induced a robust transcriptional response 45 min after stress exposure in both dorsal hippocampus (dHC) and ventral hippocampus (vHC) (see Veh-C vs Veh-S in **Fig. 1d**, **Supplementary Fig. 1a**). Prazosin only mildly impacted stress-dependent transcriptional changes in the dHC and vHC (see Veh-S vs Pra-S in **Fig. 1d**, **Supplementary Fig. 1a**). Surprisingly, in stress-exposed animals prazosin seemed to slightly amplify - rather than prevent - some stress effects (**Supplementary Fig. 1b**). In contrast, propranolol had a profound impact, preventing many of the stress-induced changes in the dHC and vHC (see Veh-S vs Pro-S in **Fig. 1d**, **Supplementary Fig. 1a**). Indeed, a direct comparison between the stress group and the stress + propranolol group found many genes that were significantly altered by propranolol administration (**Fig. 1e**, **Supplementary Fig. 1c**). This response to propranolol was very similar in the dHC and vHC (**Fig. 1e**).

While blocking β-adrenergic receptors was able to block stress-induced gene expression, we did not test whether propranolol might decrease gene expression already at baseline, independent of stress. Additionally, all tests had thus far been conducted in male mice, raising the question about potential sex differences in NA-mediated transcriptomic responses. To address these two issues, we repeated the experiment in both sexes and included a group that received a propranolol injection but was not exposed to stress (**Fig. 1f**). Combining the data from both experiments, we repeated the analysis for each region, to identify genes whose response to stress was inhibited by propranolol (**Figure 1g**). As in the previous experiment, we found that many of the stress-induced gene expression changes were blocked by propranolol injection in both dHC (**Figure 1g**, left panel) and vHC (**Figure 1g**, right panel). Importantly, propranolol did not change the expression level of these genes in the absence of stress. We then directly compared the genes sensitive to stress and propranolol treatment in both dHC and vHC. To this end, we plotted the union of genes showing a significant stress:propranolol interaction in either region in one heatmap across both dHC and vHC (**Supplementary Figure 1d**). This showed again that the stress-induced changes were very similar in dHC and vHC, and that propranolol similarly blocked many of them. Finally, we asked whether the response differs between males and females. Despite clear sex differences in gene expression at baseline (data not shown), we found no significant sex differences in response to stress or propranolol between male and female mice (FDR<0.05; **Fig. 1g**). To more directly visualize this, we compared females and males by plotting the log2-fold changes of the stress:propranolol interaction across all stress-induced genes that were blocked by propranolol. We find very similar regulation patterns in both sexes (**Figure 1h**). Although none of these sex differences are significant, some genes seem to show quantitative differences, so we

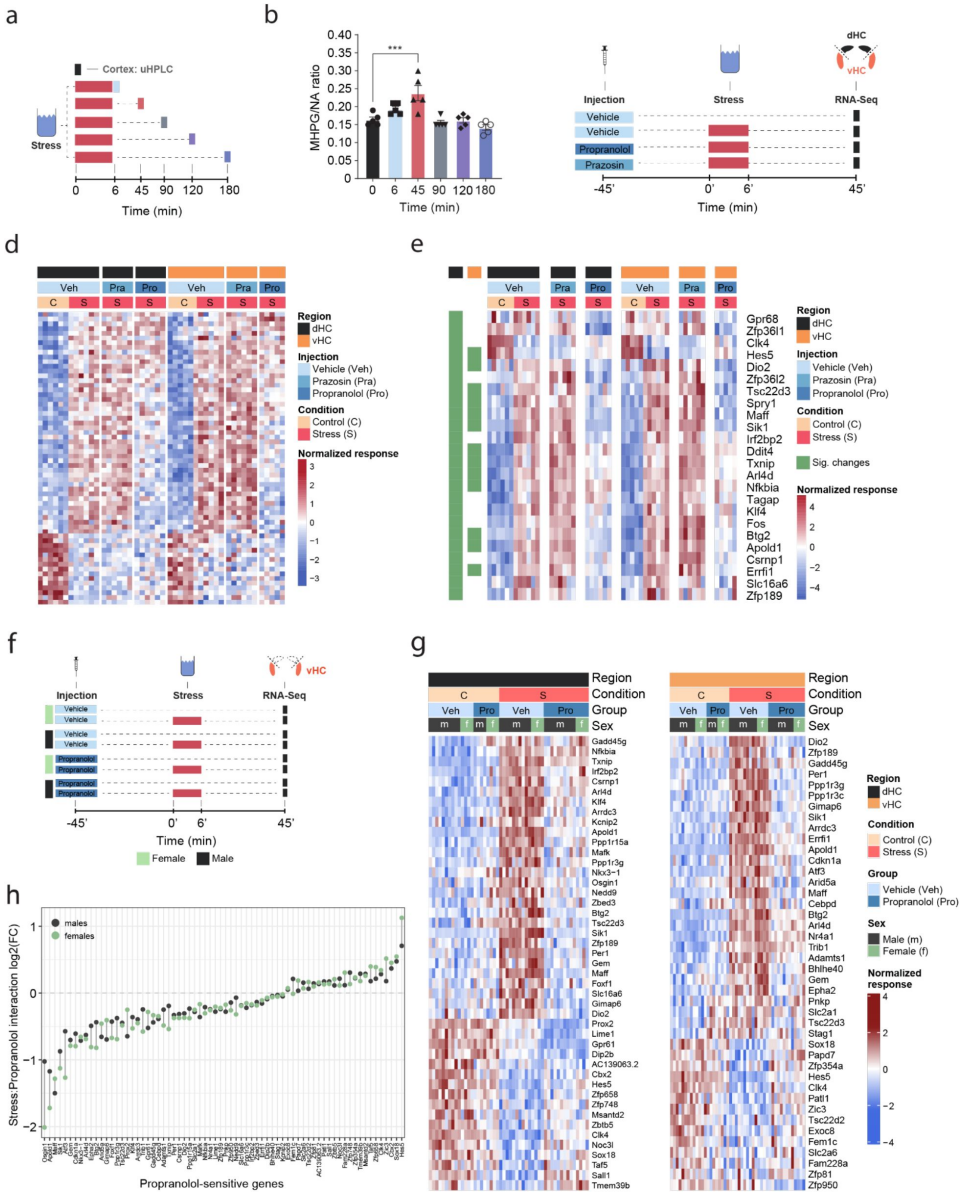


## Fig. 1

### β-adrenergic receptors mediate stress-induced transcriptomic changes in the hippocampus and are independent of subregion and sex.

**a**, Experimental design for assessing stress-induced cortical noradrenaline (NA) turnover at various time points following stress exposure. **b**, Stress-dependent changes in cortical NA turnover, as measured by the ratio of 3-Methoxy-4-hydroxyphenylglycol (MHPG) and NA levels. NA turnover significantly increased within 45 min and returned to baseline within 90 min of stress onset (one-way ANOVA with Tukey's post hoc tests; $F(5, 24) = 10.55$, $p < 0.0001$). $n = 5$ per group and individual data points are shown with bars representing mean ± s.e.m. **c**, Experimental design for assessing the effect of prazosin (Pra, 1 mg/kg, i.p.) and propranolol (Pro, 10 mg/kg, i.p.) on stress-dependent transcriptomic changes in the dorsal (dHC) and ventral (vHC) hippocampus 45 min after stress exposure. **d**, Heatmap showing all differentially expressed genes across dHC and vHC and pharmacological treatments 45 min after acute swim stress exposure. $n = 6$ per group. **e**, Heatmap selectively showing those stress-responsive genes that are affected by the β-adrenergic receptor antagonist propranolol 45 min after acute swim stress exposure in the dHC and vHC (FDR-adjusted $p < 0.05$). **f**, Experimental design for assessing propranolol-dependent changes in the vHC of female and male mice. $n = 5$ per group. **g**, Heatmap showing - across the two experiments - the expression of all stress-dependent genes that are affected by propranolol treatment in either region (dHC and vHC; FDR-adjusted $p < 0.05$). **h**, Comparison of the modulating effect of propranolol on the stress response (log2-fold-changes of the stress:propranolol interaction term) in males and females, across both experiments and regions.

plotted the expression patterns of the 5 genes showing the largest difference in interaction term as box-plots, which suggest that these spurious differences are likely due to noisy coefficient estimates (**Supplementary Fig. 1e**). To address concerns that our analysis of sex differences might not have been sufficiently powered, we performed a meta-analysis of the experiments shown here along with previously published datasets from our lab (Floriou-Servou et al. 2018; von Ziegler et al. 2022). In all these experiments, the vHC of male and female mice was profiled 45 min after exposure to an acute swim stress challenge. This resulted in a sample size of 51 males and 20 females. Despite this high number of independent samples, we could not identify any statistically significant interaction between sex and the stress response. To identify candidates that might not reach significance while discounting differences due to noise in fold-change estimates, we reproduced the same analysis using DESeq2 with Approximate Posterior Estimation for generalized linear model (apeglm) logFC shrinkage (A. Zhu, Ibrahim, and Love 2018). This analysis also did not reveal any sex differences in the stress response (**Supplementary Fig. 1f**). We then tailored the meta-analysis specifically to the set of stress-responsive genes that were blocked by propranolol, and also for these genes the response to stress was strikingly similar in both sexes (**Supplementary Fig. 1g**). Altogether, we conclude that there are no major sex differences in the rapid transcriptomic stress response in the hippocampus, and that blocking beta-receptors prevents a large set of stress-induced genes in both females and males.

We then tested whether direct activation of hippocampal β-adrenergic receptors is sufficient to induce gene expression changes. To this end, we infused animals with the β-adrenergic receptor agonist isoproterenol into the dHC (because it is easier to target than the vHC). We then manually selected a few genes whose stress-induced induction was blocked by propranolol pre-treatment either partially (*Apold1*), or completely (*Dio2*, *Sik1* and *Ppp1r3c*; see **Figure 1g**), and assessed the expression of these genes by targeted qRT-PCR assays (**Supplementary Fig. 1h**). Isoproterenol directly increased hippocampal expression of *Apold1*, *Dio2* and *Sik1*, *but not Ppp1r3c* (**Supplementary Fig. 1i**). In summary, the results presented here show that for a large number of genes, NA signaling via β-adrenergic receptors is required to regulate the stress-induced transcriptional response.

An acute stress exposure triggers the release of a plentitude of stress mediators - neurotransmitters, peptides and hormones - that interact to regulate molecular changes (Joëls and Baram 2009). As it is unclear how NA interacts with other stress mediators, we asked whether we could isolate the molecular changes for which NA release is not only required, but sufficient, by triggering NA release in the hippocampus. Because hippocampal NA supply is provided exclusively by long-range projections from the LC (Loy et al. 1980; Robertson et al. 2013; Oleskevich, Descarries, and Lacaille 1989), we first pharmacologically activated NA release using the α2-adrenergic receptor antagonist yohimbine, which strongly disinhibits noradrenergic neurons (**Fig. 2a**). As expected, systemic administration of yohimbine (3 mg/kg, i.p.) led to a strong increase in cFos expression within the LC (**Fig. 2b**) and increased NA turnover in the cortex (**Supplementary Fig. 2a**). Because NA mediates the stress-induced increase in anxiety (McCall et al. 2015; Zerbi et al. 2019), we also evaluated behavioral changes in the open field test. We had shown previously that acute stress increases anxiety in the open field test (Sturman, Germain, and Bohacek 2018; von Ziegler et al. 2022) (**Supplementary Fig. 3a**), and very similarly yohimbine also suppressed locomotion and exploratory behaviors (**Supplementary Fig. 3b**). To directly compare the impact of stress and yohimbine injection on the transcriptomic response in the hippocampus, we then exposed mice to acute swim stress, or to yohimbine injection without stress exposure (**Fig. 2c**). Yohimbine induced a clear and consistent transcriptional response in the dHC and vHC. Direct comparison between stress and yohimbine revealed no significant differences (**Fig. 2d-e**, **Supplementary Fig. 2b**), suggesting that yohimbine administration alone can mimic a large fraction of the stress-induced transcriptional response. To more specifically probe whether selective activation of the LC-NA system alone is sufficient to trigger the observed changes in gene expression, we turned to direct activation of the LC. First, we used the chemogenetic actuator hM3Dq (H. Zhu et al. 2016) to trigger a strong and

prolonged activation of the LC (**Fig. 2f**). In support of previous work (Zerbi et al. 2019; Privitera et al. 2020), injection of an ultra-low dose of the potent hM3Dq-actuator clozapine (0.03 mg/kg) led to a strong cFos increase in tyrosine hydroxylase (TH) positive LC neurons in hM3Dq+, but not in hM3Dq-animals (**Fig. 2g**). Further, we used fiber photometry combined with genetically encoded NA sensors to measure NA release in real time directly in the hippocampus (Kagiampaki et al. 2023; Grimm et al. 2022; Feng et al. 2019). We found that chemogenetic LC activation leads to a rapid and sustained increase in hippocampal NA in both females and males (**Supplementary Figure 2c-e**).

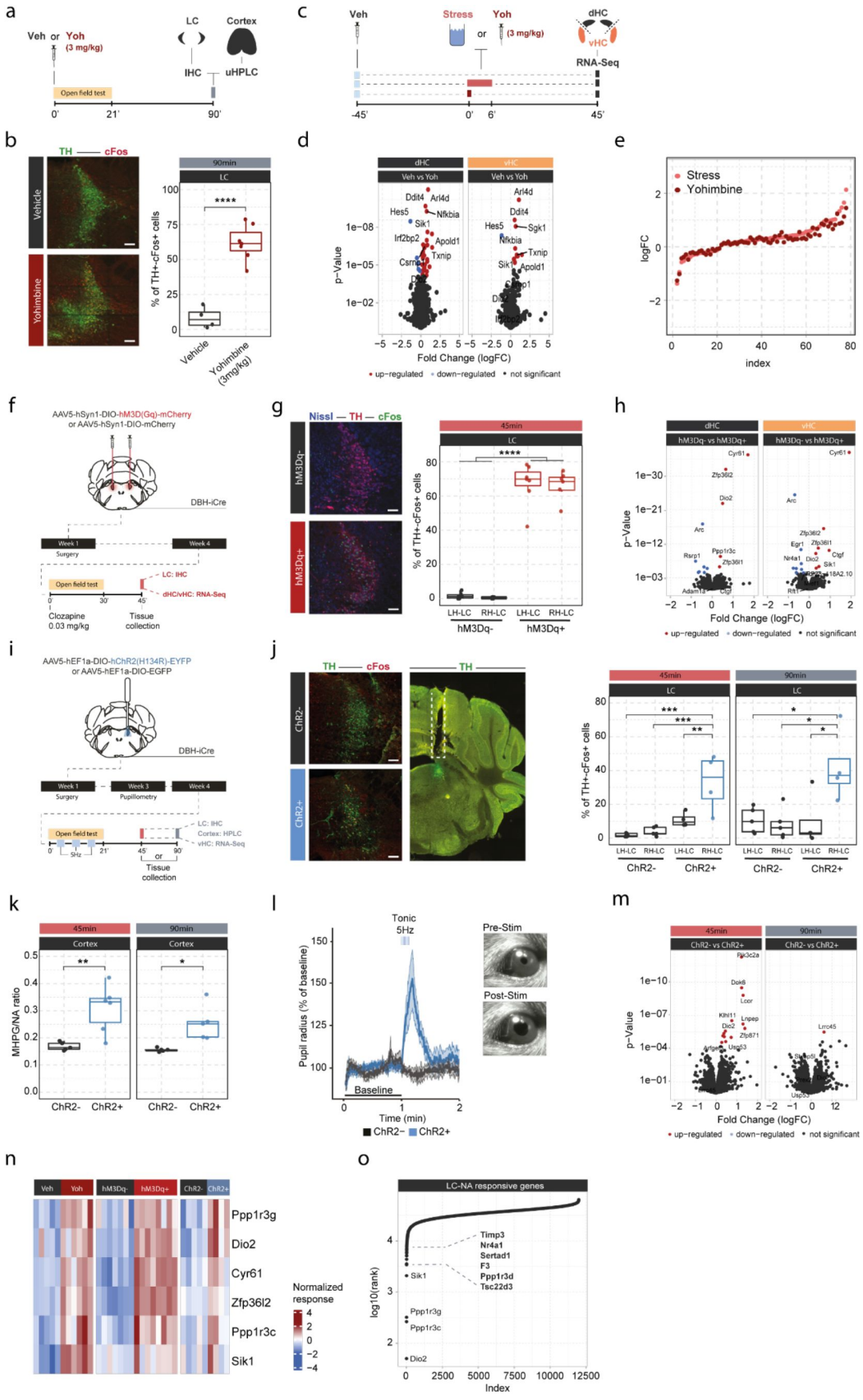
a
Veh or Yoh
(3 mg/kg)
LC
Cortex
IHC
uHPLC
Open field test
0'
21'
90'
c
Veh
Stress
Yoh
(3 mg/kg)
or
dHC
vHC
RNA-Seq
-45'
0'
6'
45'
b
TH — cFos
Vehicle
Yohimbine
90min
LC
% of TH+cFos+ cells
Vehicle
Yohimbine (3mg/kg)
d
dHC
vHC
Veh vs Yoh
p-Value
Fold Change (logFC)
up-regulated
down-regulated
not significant
e
Stress
Yohimbine
logFC
index
f
AAV5-hSyn1-DIO-hM3D(Gq)-mCherry
or AAV5-hSyn1-DIO-mCherry
DBH-iCre
Week 1
Surgery
Week 4
LC: IHC
Open field test
dHC/vHC: RNA-Seq
Clozapine
0.03 mg/kg
Tissue
collection
g
Nissl — TH — cFos
hM3Dq-
hM3Dq+
45min
LC
% of TH+cFos+ cells
LH-LC
RH-LC
h
dHC
vHC
hM3Dq- vs hM3Dq+
p-Value
Fold Change (logFC)
i
AAV5-hEF1a-DIO-hChR2(H134R)-EYFP
or AAV5-hEF1a-DIO-EGFP
DBH-iCre
Week 1
Surgery
Week 3
Pupillometry
Week 4
LC: IHC
Cortex: HPLC
vHC: RNA-Seq
Open field test
5Hz
or
Tissue
collection
j
TH — cFos
TH
ChR2-
ChR2+
45min
90min
LC
% of TH+cFos+ cells
k
45min
90min
Cortex
MHPG/NA ratio
l
Tonic
5Hz
Pre-Stim
Post-Stim
Pupil radius (% of baseline)
Baseline
Time (min)
ChR2- ChR2+
m
45min
90min
ChR2- vs ChR2+
p-Value
Fold Change (logFC)
n
Veh
Yoh
hM3Dq-
hM3Dq+
ChR2-
ChR2+
Ppp1r3g
Dio2
Cyr61
Zfp36l2
Ppp1r3c
Sik1
Normalized
response
o
LC-NA responsive genes
log10(rank)
Index
Timp3
Nr4a1
Sertad1
F3
Ppp1r3d
Tsc22d3
Sik1
Ppp1r3g
Ppp1r3c
Dio2

**Fig. 2**

**Locus Coeruleus-mediated transcriptomic changes in the hippocampus.**

**a**, Experimental design for assessing LC activation and cortical NA release induced by injection of yohimbine (3 mg/kg, i.p.). **b**, Representative images and quantification of LC activation in mice 90 min after injection of vehicle or yohimbine as measured by cFos (red) and tyrosine hydroxylase (TH, green) coexpression within LC neurons. Yohimbine injection increased cFos expression within LC neurons compared to vehicle-injected animals (unpaired t test; t(8.9) = −8.814, $p$ = 1.083e-05). Vehicle, $n$ = 4; Yohimbine $n$ = 7. Scale bar: 100µm. **c**, Experimental design for comparing molecular changes in the hippocampus after acute swim stress exposure or yohimbine administration. **d**, Volcano plots showing differentially expressed RNA transcripts in the dorsal (dHC) and ventral (vHC) hippocampus between control (Veh) and yohimbine (Yoh) injected animals 45 min after injection. Red and blue values represent changes with FDR-adjusted $p$<0.05 (Veh $n$ = 6, Yoh $n$ = 6). **e**, Strength of the yohimbine effect in comparison to the transcriptomic stress response. Data are sorted by interaction strength in the stress group (orange) and the corresponding interaction strength of the yohimbine group are shown in dark red for the same gene. **f**, Experimental design for assessing LC activation and hippocampal transcriptomic changes induced by chemogenetic LC activation. **g**, Representative images and quantification of LC activation in mice 45 min after injection of clozapine (0.03 mg/kg) in hM3Dq- and hM3Dq+ animals as measured by cFos (green) and tyrosine hydroxylase (TH, red) coexpression within LC neurons. Neurons are stained with Nissl (blue). Clozapine injection increased cFos expression within LC neurons in hM3Dq+ animals compared to hM3Dq-animals (one way ANOVA; F(3, 23) = 135.4, $p$ = 9.34e-15). hM3Dq-$n$ = 6, hM3Dq+ $n$ = 7. Scale bar: 100µm. **h**, Volcano plots showing differentially expressed RNA transcripts between hM3Dq- and hM3Dq+ animals 45 min after injection of clozapine (0.03 mg/kg) in the dHC and vHC. Red and blue values represent changes with FDR-adjusted $p$<0.05 (hM3Dq- $n$ = 6, hM3Dq+ $n$ = 7). **i**, Experimental design for assessing LC activation, cortical NA release, pupillometry and hippocampal transcriptomic changes induced by optogenetic 5 Hz LC activation. **j**, Representative images and quantification of LC activation in mice after 5 Hz optogenetic LC activation as measured by cFos (red) and tyrosine hydroxylase (TH, green) coexpression within LC neurons in stimulated and non-stimulated LC hemispheres of ChR2- and ChR2+ animals. 5 Hz stimulation increased cFos expression within LC neurons in stimulated LC hemispheres of ChR2+, but not in ChR2-animals 45 min (one-way ANOVA with Tukey's post hoc tests; F(3, 14) = 12.91, $p$ = 0.000256) and 90 min after stimulation onset (one way ANOVA with Tukey's post hoc tests; F(3, 14) = 5.866, $p$ = 0.00824). ChR2- (45 min), $n$ = 5; ChR2- (90 min), $n$ = 5; ChR2+ (45 min), $n$ = 4; ChR2+ (90 min), $n$ = 4. Scale bar: 100µm. **k**, Quantification of cortical MHPG/NA ratio, as measured by uHPLC, after 5 Hz optogenetic LC activation in ChR2- and ChR2+ animals. 5 Hz stimulation increased cortical NA turnover in ChR2+ animals (unpaired t test; 45 min: t(3.6) = 8.444, $p$ = 0.001681; 90 min: t(4.0854) =3.4127, $p$ = 0.02608). ChR2-45min, $n$ = 5; ChR2-90min, $n$ = 5; ChR2+ 45min, $n$ = 6; ChR2+ 90min, $n$ = 5. **l**, Average pupil size changes in response to 5 Hz optogenetic LC activation in ChR2- and ChR2+ animals. 5 Hz stimulation increased pupil size in ChR2+, but not ChR2-animals. **m**, Volcano plots showing differentially-expressed RNA transcripts between ChR2- and ChR2+ animals 45 and 90 min after 5 Hz optogenetic LC activation in the ventral (vHC) hippocampus. Red and blue values represent changes with FDR-adjusted $p$<0.05 (ChR2- $n$ = 10, ChR2+ $n$ = 11). **n**, Heatmap showing genes that are commonly differentially expressed by yohimbine, chemogenetic and optogenetic induced LC activation. **o**, Logarithmic cumulative rank of genes across all experiments from **figure 1** and **2** in terms of their NA responsiveness. A lower cumulative rank indicates that a gene is among the more significant hits across all analyses (for full list of included analyses see methods). Labels indicate the 10 genes identified to be most responsive to LC-NA stimulation. *$p$ < 0.05, **$p$ < 0.01, ***$p$ < 0.001, ****$p$ < 0.0001.

Behaviorally, chemogenetic LC activation induced an anxiety-like phenotype in the open field test, similar to the response to yohimbine (**Supplementary Fig. 3c**). Transcriptomic analysis revealed that chemogenetic LC activation induced significant transcriptomic changes that were similar in the dHC and vHC (**Fig. 2h**). Overall, these transcriptional changes affected fewer genes than those observed after systemic noradrenergic activation by yohimbine administration.

Despite its specificity, chemogenetic LC activation does not provide the temporal control to restrict LC activation to shorter periods of time. Thus, we repeated the experiment using optogenetic LC activation (**Fig. 2i**). To demonstrate that optogenetic LC activation directly triggers NA release in the hippocampus, we combined it with fiber photometry recordings using NA sensors (**Supplementary Figure 2f**). We found that short (10 sec) activation with 5 Hz triggered an almost instantaneous, sharp increase in hippocampal NA release in both females and males (**Supplementary Figure 2g-h**). To mimic stress-induced LC activity, LC neurons were unilaterally stimulated with 5 Hz in a 3 min off/on paradigm for 21 min, which has previously been shown to phenocopy stress-induced effects on behavior in mice (McCall et al. 2015, 2017). Again, tissue was collected 45 min after the start of stimulation, and in a separate cohort also 90 min afterwards, to study how LC-mediated transcriptomic responses evolve over time. Optogenetic LC activation led to a significant cFos increase only in the stimulated LC hemisphere of ChR2+ animals, and these changes were significant at both time points (**Fig. 2j**). Stimulated ChR2+ animals also showed a significant increase in the MHPG/NA ratio 45 and 90 min after stimulation onset compared to controls (**Fig. 2k**). Additionally, we found that tonic 5 Hz activation of the LC led to immediate pupil dilation in ChR2+, but not in ChR2-animals (**Fig. 2l**), as previously described (Privitera et al. 2020). Unilateral 5 Hz stimulation also reduced exploratory rearing behaviors in ChR2+ animals in the open field test (**Supplementary Fig. 3d**). Similar to the effects of acute stress and chemogenetic LC activation, unilateral 5 Hz stimulation of the LC induced significant transcriptomic changes at the 45 min time point in the ipsilateral vHC of ChR2+ mice compared to controls (**Fig. 2m**). Notably, most of these changes disappeared again 90 min after stimulation onset, indicating that the LC-NA system mainly induces an early wave of transcriptomic changes in the hippocampus, which are not maintained over longer periods of time.

Next, we leveraged the extensive transcriptional data presented thus far to test which genes were consistently responsive to the various manipulations of the LC-NA system across experiments. First, we compared gene expression changes induced by yohimbine, chemogenetic and optogenetic LC activation in the vHC. This allowed us to identify a small set of genes that are very consistently regulated across all modes of LC activation (**Fig. 2n**). Second, we ranked genes across all the transcriptomic experiments according to their responsiveness to NA manipulations (based on p-value). This analysis includes acute stress exposure with pharmacological inhibition of NA receptors, as well as yohimbine treatment, chemogenetic and optogenetic LC activation. We then calculated the cumulative rank for each gene across all experiments to find genes with the most consistent response to NA manipulations (Supplementary Table 1). This analysis reproduced most of the genes identified in **Figure 2n**, and additionally revealed more genes with particularly robust changes in response to LC-NA manipulations across experiments (**Fig. 2o**, **Supplementary Fig. 4**). The top 10 genes were *Dio2*, *Ppp1r3c*, *Ppp1r3g*, *Sik1*, *Tsc22d3*, *Ppp1r3d*, *F3*, *Sertad1*, *Nr4a1* and *Timp3*. For visualization, the top 4 of these genes are shown across all LC-NA manipulations in **Supplementary Fig. 4**. Going forward, we use these 10 transcripts as a *bona fide* list of LC-NA-responsive genes.

Our optogenetic data have demonstrated that LC neurons engage transcriptomic responses when firing at 5 Hz. Recent work has suggested that the effects of LC stimulation on brain processes, from behavior to brain network activity, depend on the firing pattern and frequency of the LC (Harley and Yuan 2021; Ghosh et al. 2021; Grimm et al. 2022). To investigate if the molecular responses would differ between these stimulation conditions, we optogenetically activated the LC using two tonic paradigms (3 and 5 Hz), and one phasic paradigm (15 Hz, see schematic in **Fig. 3a**). Stimulation was again conducted unilaterally in a 3 min off/on paradigm for 21 minutes for each of the stimulation groups, and tissue was collected for RNA-sequencing 45 min after stimulation onset (**Fig. 3a**). To increase statistical power in the face of higher variability due to the relatively small sample sizes (n=5-6 mice per group), we restricted our analysis to the ten most LC-NA-responsive genes identified earlier. Surprisingly, we found that expression of these genes was similarly affected by tonic 3 Hz, 5 Hz and phasic 15 Hz LC stimulation (**Fig 3b**). These

findings suggest that in contrast to circuit-wide changes, the molecular consequences to NA release are independent of the firing intensity and activity pattern of the LC neurons. While these transcriptomic changes seem to depend on LC-NA activity, our approach so far was not able to resolve whether NA mediates gene expression via direct effects within the hippocampus. Specifically, due to the widespread projections of the LC, it is possible that activation of other brain regions or other neurotransmitter systems might have led to indirect regulation of gene expression in the hippocampus. Thus, we selectively targeted only a subpopulation of LC neurons projecting to the hippocampus ($LC_{HC}$) using a unilateral, retrograde optogenetic approach (**Fig. 3c**). Retrograde virus expression was restricted to dorsomedially located LC neurons ipsilateral to the injection site (**Fig. 3d**), as previously described (Robertson et al. 2013). To confirm successful $LC_{HC}$ stimulation, we directly assessed NA turnover in the cortex and dHC. Indeed, 5Hz stimulation of $LC_{HC}$ neurons led to an increased MHPG/NA ratio 45 min after stimulation onset in the ipsilateral dHC but not in the cortex (**Fig. 3e**). In addition, 5 Hz stimulation of $LC_{HC}$ neurons did not impact pupil size, emphasizing the modular organization of the LC (**Fig. 3f**). Within the vHC of the same animals we then assessed the transcriptional impact of targeted $LC_{HC}$ 5 Hz activation on the top ten NA-sensitive genes in the vHC at the 45 min time point. Indeed, activation of hippocampus-projecting LC neurons affected most target genes, including *Dio2*, *Ppp1r3c* and *Ppp1r3g* (**Fig. 3g-h**).

To understand in more detail how these NA-sensitive genes are affected by different stressors, we investigated whether the expression of *Dio2, Ppp1r3c, Ppp1r3g, Sik1* and *Nr4a1* is specific to acute swim stress exposure or independent of the stress context. Therefore, we assessed their expression in a dataset comparing the effect of various stressors on the hippocampal transcriptome (Floriou-Servou et al. 2018). We found that these genes are not only upregulated by swim stress, but also by novelty stress, restraint and footshock stress (**Fig. 4b**). This suggests that expression of these genes is robustly induced by a wide range of stressors.

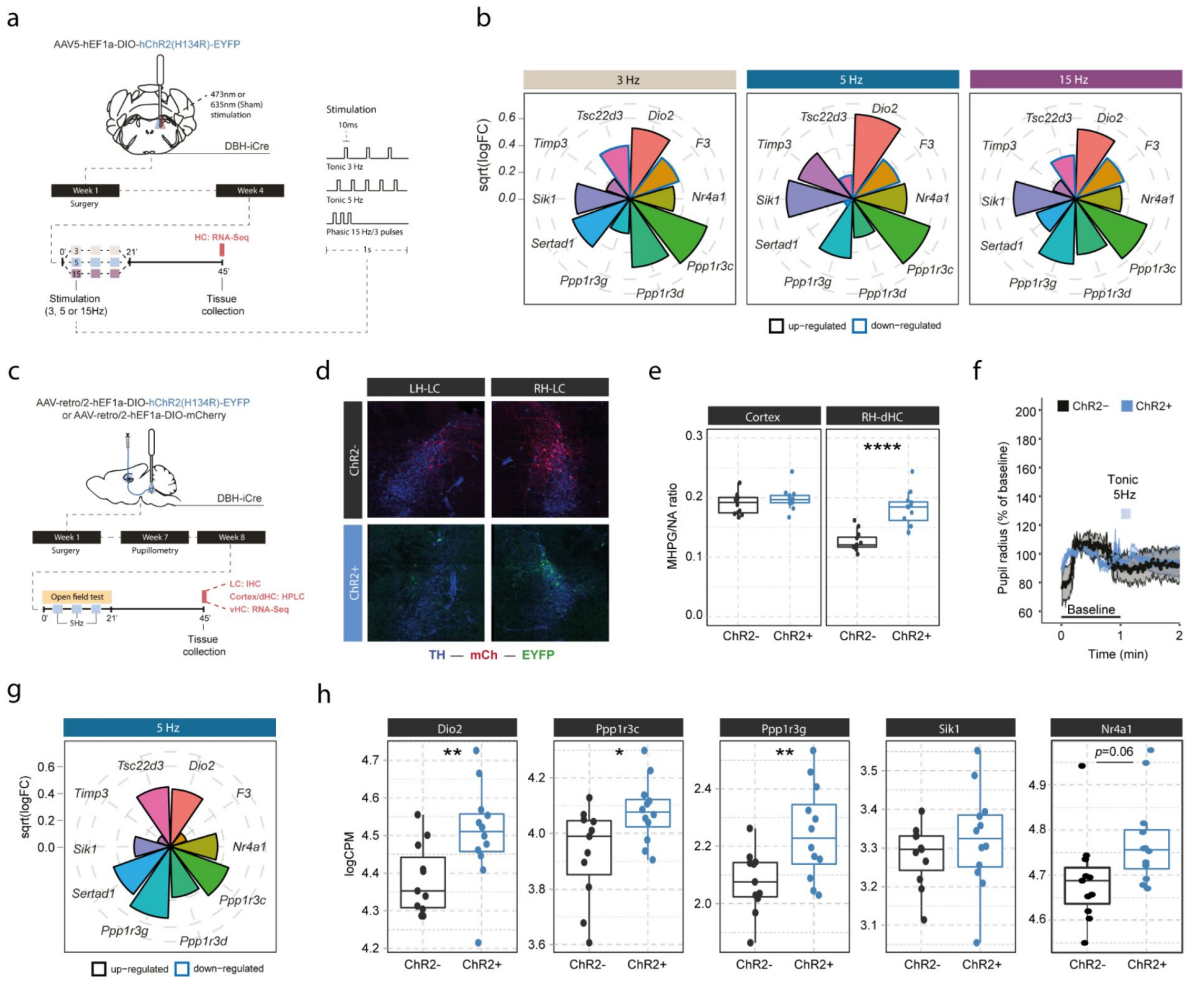


## Fig. 3

### LC-NA mediated molecular responses in the hippocampus are independent of LC firing pattern and frequency and are directly stimulated via hippocampus-projecting LC neurons.

**a**, Experimental design for assessing molecular changes in the hippocampus induced by optogenetic LC activation with tonic (3 Hz and 5 Hz) and phasic (15 Hz) firing patterns. **b**, Radial plots showing expression changes (based on the logFC) of the most LC-NA-responsive genes after optogenetic LC activation in ChR2+ animals compared to controls (Sham $n$ = 6, 3 Hz $n$ = 6, 5 Hz $n$ = 7, 15 Hz $n$ = 6). Black borders indicate that the gene is upregulated, blue border downregulated. **c**, Experimental design for assessing molecular changes in the hippocampus induced by retrograde optogenetic 5 Hz activation of hippocampus projecting LC neurons ($LC_{HC}$). **d**, Representative images of retrograde mCherry (mCh, red) and ChR2-EYFP (EYFP, green) expression in tyrosine hydroxylase (TH, blue) positive LC neurons across hemispheres. **e**, Cortical and right dorsal hippocampal (RH-dHC) NA turnover as measured by ultra-high performance liquid chromatography 45 min after 5 Hz optogenetic activation of $LC_{HC}$ neurons in ChR2- and ChR2+ animals. 5 Hz stimulation of $LC_{HC}$ neurons increased dorsal hippocampal but not cortical NA turnover in ChR2+ animals (unpaired t test; t(17.43) = −5.5997, $p$ = 2.911e-05). ChR2-, $n$ = 12; ChR2+, $n$ = 12. ****$p$ < 0.0001. **f**, Average pupil size changes in response to 5 Hz optogenetic activation of $LC_{HC}$ projecting neurons in ChR2- and ChR2+ animals. **g**, Radial plots showing expression changes (based on the logFC) of the top ten LC-NA responsive genes in response to optogenetic $LC_{HC}$ activation with tonic 5 Hz stimulation in ChR2+ animals compared to ChR2- 45 min after stimulation onset (ChR2-$n$ = 12, ChR2+ $n$ = 12). **h**, Selective boxplots of NA-responsive genes *Dio2*, *Ppp1r3c*, *Ppp1r3g*, *Sik1* and *Nr4a1* in response to 5 Hz optogenetic activation of $LC_{HC}$ projecting neurons in ChR2- and ChR2+ animals 45 min after stimulation onset. (ChR2- $n$ = 12, ChR2+ $n$ = 12). 5 Hz optogenetic activation of $LC_{HC}$ projecting neurons increased hippocampal expression of *Dio2*, *Ppp1r3c*, *Ppp1r3g* and *Nr4a1*. *$p$ < 0.05, **$p$ < 0.01, ***$p$ < 0.001, ****$p$ < 0.0001.

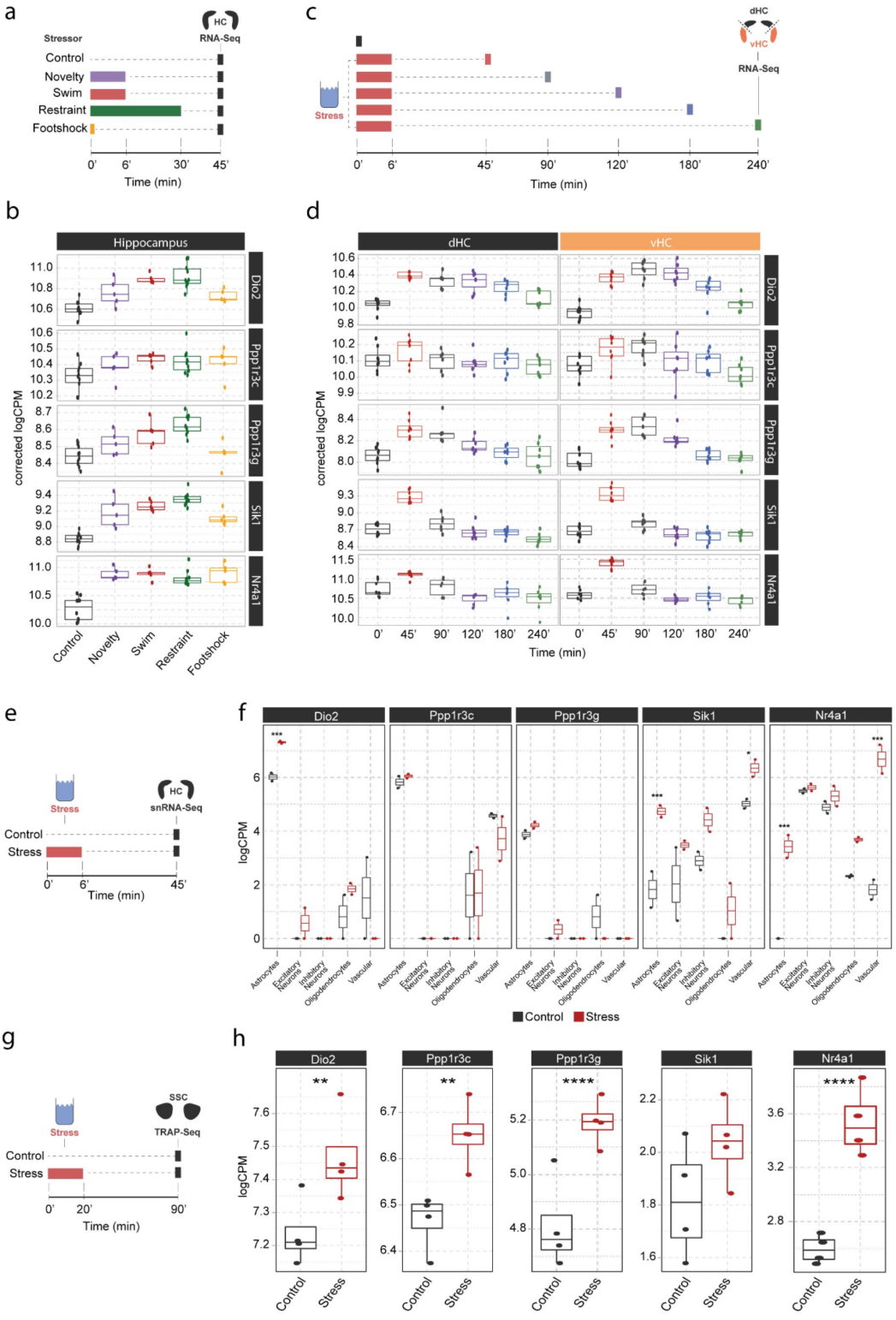
a
Stressor
HC
RNA-Seq
Control
Novelty
Swim
Restraint
Footshock
0'
6'
30'
45'
Time (min)
c
dHC
vHC
RNA-Seq
Stress
0'
6'
45'
90'
120'
180'
240'
Time (min)
b
Hippocampus
Dio2
Ppp1r3c
Ppp1r3g
Sik1
Nr4a1
corrected logCPM
Control
Novelty
Swim
Restraint
Footshock
d
dHC
vHC
corrected logCPM
Time (min)
e
Stress
HC
snRNA-Seq
Control
Stress
0'
6'
45'
Time (min)
f
Dio2
Ppp1r3c
Ppp1r3g
Sik1
Nr4a1
logCPM
Astrocytes
Excitatory Neurons
Inhibitory Neurons
Oligodendrocytes
Vascular
Control
Stress
g
Stress
SSC
TRAP-Seq
Control
Stress
0'
20'
90'
Time (min)
h
Dio2
Ppp1r3c
Ppp1r3g
Sik1
Nr4a1
logCPM
Control
Stress

**Fig 4.**

**Screening of publicly available datasets shows that the noradrenaline-regulated genes *Dio2, Ppp1r3c, Ppp1r3g, Sik1* and *Nr4a1* are induced by various stressors predominantly in astrocytes.**

**a**, Experimental design for assessing transcriptomic changes in the hippocampus induced by different stressors as performed by (Floriou-Servou et al. 2018). These stressors included a 10 min exposure to the open field test (Novelty), a 6 min cold swim stress (Swim), a 30 min immobilization stress (Restraint) and exposure to a 1 mA footshock (Footshock). **b**, Selective boxplots of top NA-responsive genes *Dio2*, *Ppp1r3c*, *Ppp1r3g*, *Sik1* and *Nr4a1* in response to different stressors. Control $n = 10$, Novelty $n = 5$, Swim $n = 5$, Restraint $n = 10$, Footshock $n = 5$. **c**, Experimental design for assessing transcriptomic changes in the dorsal and ventral hippocampus across 4 hours following acute swim stress exposure as performed by von Ziegler et. al. **d**, Selective boxplots showing expression changes of top NA-responsive genes *Dio2*, *Ppp1r3c*, *Ppp1r3g*, *Sik1* and *Nr4a1* across 4 hours following acute swim stress exposure. Control $n = 8$, 45 min $n = 8$, 90 min $n = 7$, 120 min $n = 7$, 180 min $n = 7$, 240 min $n = 7$. **e**, Experimental design for assessing single cell transcriptomic changes in the hippocampus 45 min following acute swim stress exposure by single-nucleus RNA sequencing as performed by von Ziegler et. al (von Ziegler et al. 2022). **f**, Selective boxplots showing expression changes of top NA-responsive genes *Dio2*, *Ppp1r3c*, *Ppp1r3g*, *Sik1* and *Nr4a1* across cell types of the hippocampus 45 min following acute swim stress exposure. Control $n = 2$, Stress $n = 2$. **g**, Experimental design for assessing actively translated RNA in the somatosensory cortex 90 min following a 20 min acute swim stress exposure by TRAP sequencing as performed by Murphy-Royal et. al (Murphy-Royal et al. 2020). **h**, Selective boxplots of top NA-responsive genes *Dio2*, *Ppp1r3c*, *Ppp1r3g*, *Sik1* and *Nr4a1* in the somatosensory cortex 90 min following a 20 min acute swim stress exposure. Acute stress increases the binding of *Dio2*, *Ppp1r3c*, *Ppp1r3g* and *Nr4a1* mRNA to the ribosome. Control $n = 4$, Stress $n = 4$. *$p<0.05$, **$p < 0.01$, ***$p < 0.001$, ****$p < 0.0001$.

We then interrogated a recently published stress resource, which tracks stress-induced transcriptional changes over time in the hippocampus (von Ziegler et al. 2022). Across 4 hours following acute swim stress exposure, we found two distinctive expression patterns among these genes. While *Sik1* and *Nr4a1* show the characteristics of an immediate early gene with a sharp rise and fall in expression within 90 min of stress onset, upregulation of *Dio2*, *Ppp1r3c* and *Ppp1r3g* is maintained for at least 2-4 hours following stress exposure (**Fig. 4d**), suggesting that mechanisms are in place to prolong expression beyond the initial rise in NA. Reanalysis of a hippocampal single-nucleus RNA-sequencing dataset after a swim stress challenge (von Ziegler et al. 2022) revealed that stress-induced upregulation of *Dio2*, *Ppp1r3c* and *Ppp1r3g* seems predominantly restricted to astrocytes, while *Sik1* and *Nr4a1* show a broader expression among glia, neuronal and vascular cells.

Finally, to determine if these transcripts are also actively translated in astrocytes after stress exposure, we re-analyzed a dataset using translating ribosome affinity purification followed by RNA sequencing (TRAPseq) - in astrocytes of the somatosensory cortex after a similar acute swim stress paradigm as described here (Murphy-Royal et al. 2020). We found that *Dio2*, *Ppp1r3c*, *Ppp1r3g* and *Nr4a1* are significantly upregulated after stress exposure. Altogether, these results highlight that the NA-dependent gene expression changes that occur in response to stress exposures are most prominent in astrocytes.

# Discussion

## Dissecting stress with transcriptomics

The widespread molecular changes induced in the brain by an acute stress exposure (Stankiewicz et al. 2015; von Ziegler et al. 2022; Floriou-Servou et al. 2018; Mifsud et al. 2021) are part of a healthy stress response, and their dysregulation is often a hallmark of neuropsychiatric disorders (Girgenti, Pothula, and Newton 2021; Rubin, Gray, and McEwen 2014). To date, the contribution of corticosteroid signaling to stress-induced transcriptional changes has been well characterized (Mifsud et al. 2021; Gray et al. 2013; Meijer et al. 2022), yet the contribution of other stress-mediators remains unexplored. Here, we extensively characterize the contribution of noradrenergic signaling to the transcriptomic response in the hippocampus during stress. By combining transcriptomics with circuit-specific manipulation of the LC-NA system, our unbiased approach reveals a small, but highly reproducible set of genes that are regulated directly by NA release from the LC. This gene set identifies astrocytes as a key target for NA-induced transcriptional changes.

## Complex interactions between stress mediators

Our results indicate that the transcriptomic response to a natural stressor is more complex than the gene expression changes induced solely by NA. This is well in line with the notion that multiple stress-mediators contribute to the molecular response, and that these systems can also interact with each other. The response to LC-NA activation we observe in our experiments is short in duration. Following temporally-precise optogenetic LC activation, gene expression changes did resolve within 90 min. This is noticeably different from an actual stress response, where gene expression evolves over a 4-hour period (von Ziegler et al. 2022). Specifically, LC-NA regulated genes like *Ppp1r3c, Ppp1r3g* and *Dio2*, were elevated for several hours after stress exposure (**Fig. 4d**). This suggests that other stress-induced signals can also regulate these genes more slowly or with a greater delay. Indeed, a recent study reported that activation of the glucocorticoid receptor by dexamethasone can induce strong transcriptomic changes 4 hours after injection across multiple brain regions (Gerstner et al. 2022). Analyzing their data we found that *Dio2*, *Ppp1r3c* and *Ppp1r3g* were all upregulated 4 hours after dexamethasone injection. This supports the concept that NA can act as a rapid molecular regulator, whereas glucocorticoid signaling can extend these stress-induced changes over longer time periods (Hermans et al. 2014).

In contrast to the small set of genes triggered by isolated LC-NA activation, blocking β-receptors prevents the induction of a large fraction of genes normally activated by natural stressors. This suggests that even if NA release alone is not sufficient to activate large numbers of genes, it is required to enable or enhance gene expression triggered via other mechanisms. A powerful regulator of transcription is neuronal activity linked to enhanced glutamate release (Fernandez-Albert et al. 2019; Tyssowski et al. 2018). The notion that NA release could enhance glutamate-dependent transcriptional cascades is in line with physiological evidence that NA can increase the excitability of neurons (Bouret and Sara 2002), and with the "glutamate amplifies noradrenergic effects" (GANE) model, which posits that NA can amplify local glutamate release to create hot-spots of activity (Mather et al. 2016).

Finally, our observation that systemic administration of the α2-adrenergic receptor antagonist yohimbine very closely recapitulates the transcriptional response to stress stands in contrast to the much more selective transcriptional changes observed after chemogenetic or optogenetic LC-NA activation. This difference could be due to various factors. First, it remains unclear how strong the LC gets activated by yohimbine versus hM3Dq-DREADDs. However, given the potent LC activation observed after DREADD activation, it seems unlikely that yohimbine would lead to a more pronounced LC activation, thus explaining the stronger transcriptional effects. Second, contrary to LC-specific DREADD-activation, systemic yohimbine injection will also antagonize postsynaptic α2-adrenergic receptors throughout the brain (and periphery). More research is

needed to determine whether this could have a more widespread impact on the hippocampus (and other brain regions) than isolated LC-NA activation, further enhancing excitability by preventing α2-mediated inhibition of cAMP production. Finally, systemic yohimbine administration and noradrenergic activity have been shown to induce corticosterone release into the blood (Johnston, Baldwin, and File 1988; Leibowitz et al. 1988; Fink 2016). Thus, yohimbine injection could have broader transcriptional consequences, including corticosteroid-mediated effects on gene expression.

## Transcriptomic fingerprinting of NA effects using LC circuit manipulation

While systemic pharmacological treatments have been a common approach in studying the effects of different stress mediators and their receptors, they lack specificity and do not provide causal evidence that the release of a given stress mediator is sufficient to trigger molecular changes. By directly combining selective chemogenetic activation of the LC with transcriptomic analyses in the hippocampus, we were able to identify a subset of stress-responsive genes that depend on β-adrenergic signaling, and which can be triggered by NA alone in the absence of a physiological stress response. Using optogenetics we were able to validate these findings and further demonstrate that the strongest NA-mediated changes are similarly affected by tonic (3 Hz and 5 Hz) and phasic (15 Hz) LC stimulation. Interestingly, this is in contrast with our previous findings that these stimulation patterns differentially affect brain network connectivity (Grimm and Duss et al, 2022). This suggests that engagement of a transcriptomic response via β-adrenergic receptors seems common across these LC activity patterns, while changes on a network level might rely more on α1-mediated effects (Zerbi et al. 2019).

We found that direct activation of hippocampus-projecting LC neurons ($LC_{HC}$) was sufficient to increase expression of the top NA-sensitive target genes, suggesting that local NA release in the hippocampus is directly contributing to these changes during stress. While we did not extensively characterize $LC_{HC}$ neurons, our data further show that in contrast to whole LC activation with 5 Hz, $LC_{HC}$ neurons do not seem to project to the cortex, nor do they affect pupil size.

## A uniform molecular response to stress and noradrenaline release in females and males

Our results, based on a meta-analysis of large sets of transcriptomic analyses across females and males, suggest that stress triggers a transcriptomic response in the hippocampus that is independent of sex. Extensive analyses of male and female hippocampi in response to stress and propranolol also suggest that stress- and propranolol-sensitive genes show similar response profiles in both sexes. However, due to the multivariate design and our genome-wide approach, subtle changes might not have survived multiple-testing correction, particularly given that our study was not designed to track hormonal fluctuations across the estrous cycle, which is known to interact with noradrenaline signaling (Bangasser, Eck, and Ordoñes Sanchez 2019). An example is Ctla2b, which has previously been shown to be dependent on β-adrenergic signaling and to be selectively increased in females after stress exposure (Roszkowski et al. 2016). Indeed, targeted interrogation of our dataset confirms that Ctla2b is increased by stress only in females but not males, yet this effect fails to pass multiple testing correction (**Supplementary Fig. 6**). Ctla2b is also not included in the meta-analysis, as it did not pass the filtering step in our analysis pipeline due to very low baseline expression levels (see Methods). We provide a full list of genes that do not pass multiple testing correction, but still show nominally significant differences in gene expression (Supplementary Table 2). Although these changes must be treated with caution, our data allow targeted hypothesis testing of individual genes to generate leads for follow-up work.

## Genes regulated by the LC-NA system

Across experiments, our transcriptomic screening revealed a conserved set of genes (**Fig. 2o**, Supplementary Table 1) that are selectively regulated by NA from LC projections in the hippocampus following acute stress exposure. Cross-referencing our data with publicly available single-cell databases suggests that - among the top ten LC-NA sensitive genes - most are enriched in astrocytes (Endo et al. 2022; von Ziegler et al. 2022). Interestingly, immediate early genes commonly upregulated during stress and associated with neuronal activation like *Fos*, *Egr1*, *Arc*, *Dusp1* and *Npas4* (Smith et al. 1992; Benito and Barco 2015; Fernandez-Albert et al. 2019; Tyssowski et al. 2018), are not upregulated by LC stimulation (**Supplementary Fig. 5**). Taken together, our findings further add to accumulating evidence highlighting astrocytes as a direct and major cellular target of the LC-NA system (Zenger et al. 2017; O'Donnell, Ding, and Nedergaard 2015; Dienel 2017).

Within the hippocampus, astrocytic pathways are emerging as important players for learning and memory processes (Gibbs, Hutchinson, and Hertz 2008; Bohmbach et al. 2022). In fact, it is well-known that NA enhances memory consolidation (Schwabe et al. 2022; McGaugh and Roozendaal 2002), and recent work suggests that these effects are mediated by astrocytic β-adrenergic receptors (Gao et al. 2016; Iqbal et al. 2023). Our transcriptomic screens revealed *Dio2* as the most prominent target influenced by LC activity. *Dio2* is selectively expressed in astrocytes and encodes for the intracellular type II iodothyronine deiodinase, which converts thyroxine (T4) to the bioactive thyroid hormone 3,3',5-triiodothyronine (T3) and therefore regulates the local availability of T3 in the brain (Bianco et al. 2019). Enzymatic activity of DIO2 has further been shown to be increased by prolonged noradrenergic transmission through desipramine treatment in LC projection areas (Campos-Barros et al. 1994). This suggests that the LC-NA system and its widespread projections could act as a major regulator of brain-derived T3. Notably, T3-signaling plays a role in hippocampal memory formation (Rivas and Naranjo 2007; Sui et al. 2006), raising the possibility that NA-induced *Dio2* activity in astrocytes might mediate some of these effects. Our molecular screening approach also revealed that three subunits of the astrocytic protein phosphatase 1 (*Ppp1r3d*, *Ppp1r3g* and *Ppp1r3c*) respond strongly to LC-NA activity. All three subunits enhance protein phosphatase 1 mediated glycogen synthesis. Especially *Ppp1r3c* expression has been found to be a master regulator of astrocytic glycogen synthesis and has previously been linked to NA activity (Allaman, Pellerin, and Magistretti 2000; Petit et al. 2021). Another important mechanism might include regulating sodium homeostasis via the widely expressed salt-inducible kinase 1 (*Sik1*). SIK1 has been shown to respond to neuronal activity and regulate $Na^+/K^+$-ATPase activity (Jaitovich and Bertorello 2010; Huang, White, and Leenen 2012; Feldman et al. 2000; Bertorello and Zhu 2009). It was also found to detect low glucose availability and initiate gluconeogenesis in liver cells (Wang et al. 2020), a process which could also be important for noradrenergic activity in the brain. Our findings support the idea of the LC-NA system as a major regulator of brain-wide energy metabolism, stimulating astrocytic glycogen breakdown and consequently increasing energy supply to target areas (Coggan et al. 2018; Dienel 2017).

Another interesting molecular target is the Nuclear Receptor Subfamily 4 Group A Member 1 (Nr4a1), a widely expressed transcription factor that could trigger broader downstream changes. Within astrocytes, Nr4a1 activity was found to reduce oxidative stress and inflammation (Xu et al. 2015; Popichak et al. 2018) and might further regulate blood brain barrier integrity (Pan et al. 2021; Paillasse and de Medina 2015). Our re-analysis of published data showed that *Dio2*, *Ppp1r3c*, *Ppp1r3g* and *Nr4a1* are actively translated in somatosensory cortical astrocytes following acute stress exposure. It remains to be tested whether protein levels, transcription factor activity or enzymatic activity of these genes are also altered in the hippocampus, and what this ultimately means mechanistically for stress-related NA signaling.

## Summary

Overall, we provide the first genome-wide characterization of the molecular impact of NA release in vivo in the brain. The set of genes that are sensitive to NA release from the LC point to astrocytes as key molecular targets of NA during stress, and suggest that astrocytic processes involving glycogen and thyroid hormone metabolism could be key to the neuromodulatory effects of NA in the hippocampus.

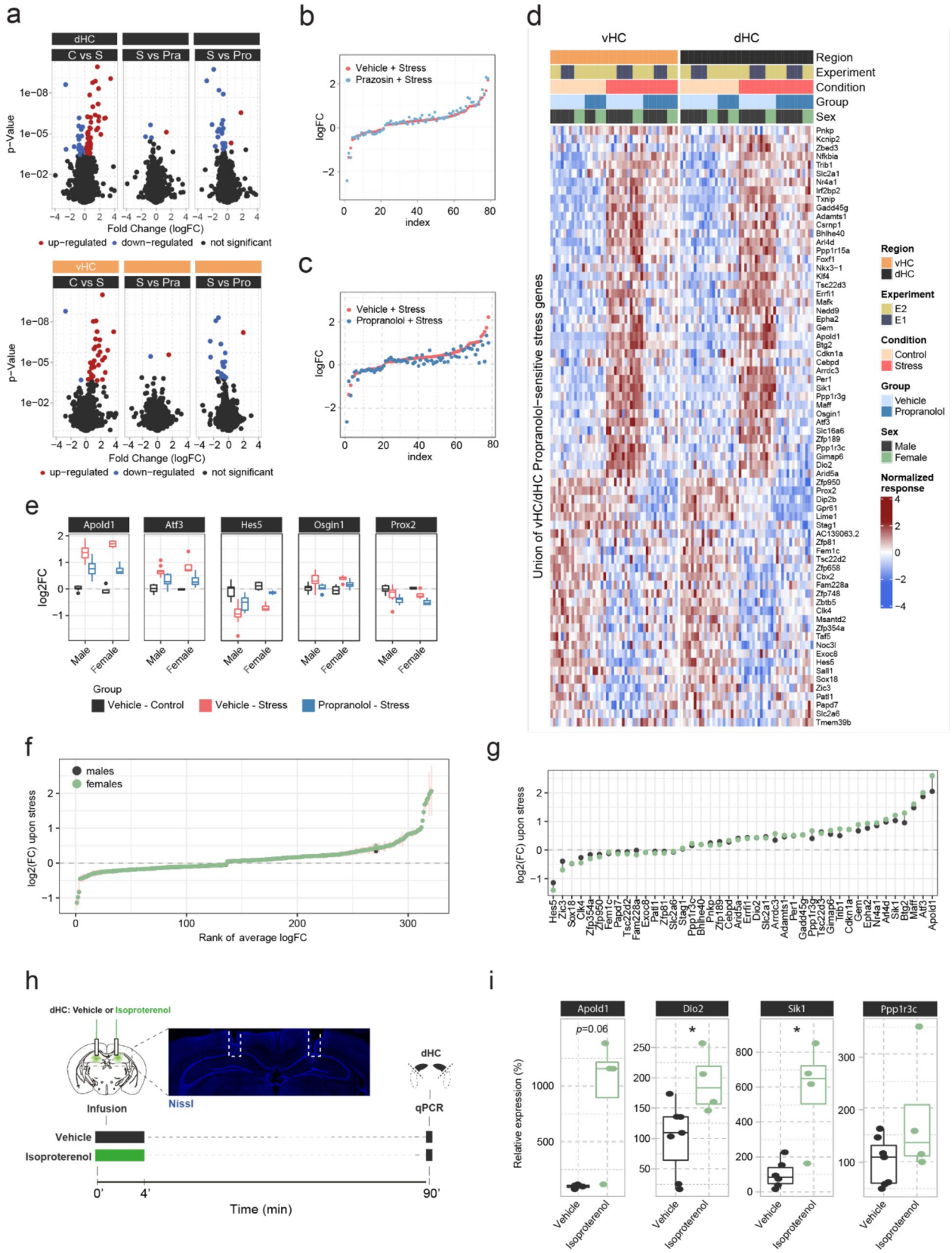
a
dHC
C vs S
S vs Pra
S vs Pro
p-Value
1e-08
1e-05
1e-02
Fold Change (logFC)
up-regulated
down-regulated
not significant
vHC
b
Vehicle + Stress
Prazosin + Stress
logFC
index
c
Vehicle + Stress
Propranolol + Stress
d
vHC
dHC
Region
Experiment
Condition
Group
Sex
Union of vHC/dHC Propranolol-sensitive stress genes
Region
vHC
dHC
Experiment
E2
E1
Condition
Control
Stress
Group
Vehicle
Propranolol
Sex
Male
Female
Normalized response
e
Apold1
Atf3
Hes5
Osgin1
Prox2
log2FC
Male
Female
Group
Vehicle - Control
Vehicle - Stress
Propranolol - Stress
f
males
females
log2(FC) upon stress
Rank of average logFC
g
log2(FC) upon stress
h
dHC: Vehicle or Isoproterenol
Nissl
dHC
Infusion
qPCR
Vehicle
Isoproterenol
0'
4'
90'
Time (min)
i
Apold1
Dio2
Sik1
Ppp1r3c
p=0.06
*
*
Relative expression (%)
Vehicle
Isoproterenol

## Supplementary Figure 1.

### In-depth analysis of noradrenergic contribution to stress-induced transcriptomic changes in the hippocampus.

**a**, Volcano plots showing differentially expressed RNA transcripts between vehicle (Veh, i.p.), prazosin (Pra, 1 mg/kg, i.p.) and propranolol (Pro, 10 mg/kg, i.p.) injected animals 45 min after onset of acute swim stress exposure. Red and blue values represent changes with FDR-adjusted $p<0.05$ ($n = 6$ per group). **b**, Strength of the prazosin effect on the transcriptomic stress response. Data are sorted by interaction strength in the stress group (orange) and the corresponding interaction strength of the stress+prazosin group are shown in lightblue for the same gene. **c**, Strength of the propranolol effect on the transcriptomic stress response. Data are sorted by interaction strength in the stress group (orange) and the corresponding interaction strength of the stress+prazosin group are shown in dark blue for the same gene. **d**, Heatmap showing expression, across both experiments and regions, of all stress genes with a significant stress:propranolol interaction. **e**, Expression (in the vHC) of the genes from **Figure 1h** showing the largest differences (none statistically significant) in the stress:propranolol interaction term between males and females. **f**, Comparison of the transcriptomic changes 45min after stress between males and females, in a meta-analysis of 71 vHC samples. The fold-change estimates were obtained using DESeq2 with apeglm-shrinkage (A. Zhu, Ibrahim, and Love 2018). Vertical bars show the standard error of the fold-change estimates. **g**, (Unshrunk) fold-change estimates of propranolol-sensitive genes upon stress in males and females, based on the meta-analysis. **h**, Experimental design for assessing the effect of intrahippocampal infusion of isoproterenol (3 µg/hemisphere) on expression of selected genes in the dorsal hippocampus (dHC) 90 min after infusion in the absence of stress. Representative image shows the cannula placement (dashed line) in the dHC stained by Nissl (blue) **i**, Boxplots showing the expression of selected stress- and propranolol-responsive genes (*Apold1, Dio2 and Sik1*) 90 min after infusion of isoproterenol (3 µg/hemisphere) into the dHC, as measured by quantitative real-time PCR. Isoproterenol increased the expression of *Dio2* (unpaired t test; $t(9) = 2.637$, $p = 0.02706$) and *Sik1* (welch unpaired t test; $t(3.3) = 3.176$, $p = 0.04428$). Vehicle, $n = 7$; Isoproterenol, $n = 4$. $^*p < 0.05$.

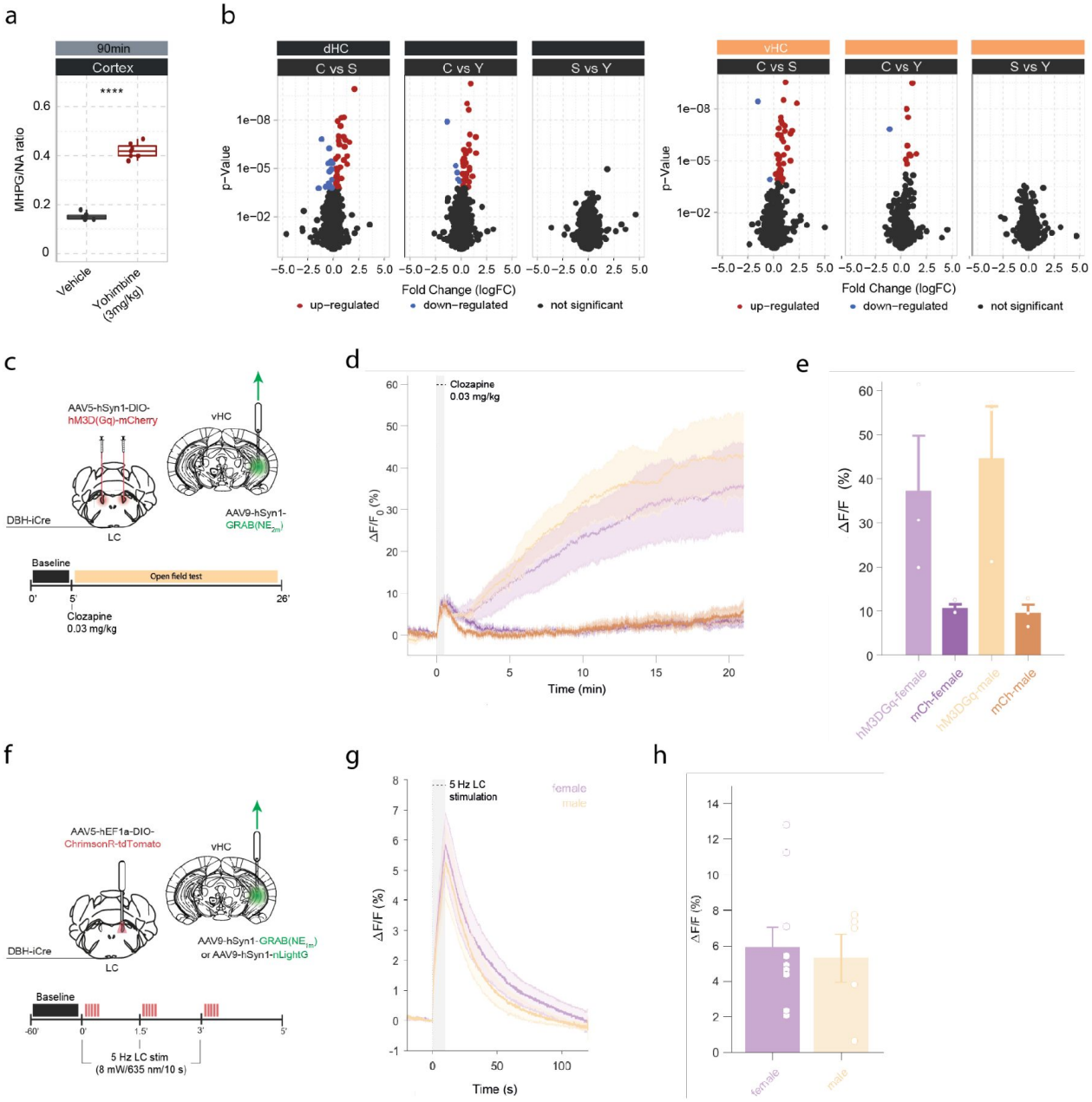
a
90min
Cortex
****
MHPG/NA ratio
0.6
0.4
0.2
0
Vehicle
Yohimbine (3mg/kg)
b
dHC
C vs S
C vs Y
S vs Y
vHC
C vs S
C vs Y
S vs Y
p-Value
1e-08
1e-05
1e-02
−5.0 −2.5 0.0 2.5 5.0
Fold Change (logFC)
up-regulated
down-regulated
not significant
c
AAV5-hSyn1-DIO-hM3D(Gq)-mCherry
vHC
DBH-iCre
LC
AAV9-hSyn1-GRAB(NE2m)
Baseline
Open field test
0'
5'
26'
Clozapine 0.03 mg/kg
d
Clozapine 0.03 mg/kg
ΔF/F0 (%)
Time (min)
e
ΔF/F (%)
hM3DGq-female
mCh-female
hM3DGq-male
mCh-male
f
AAV5-hEF1a-DIO-ChrimsonR-tdTomato
vHC
DBH-iCre
LC
AAV9-hSyn1-GRAB(NE1m) or AAV9-hSyn1-nLightG
Baseline
-60'
0'
1.5'
3'
5'
5 Hz LC stim (8 mW/635 nm/10 s)
g
5 Hz LC stimulation
female
male
ΔF/F (%)
Time (s)
h
ΔF/F (%)
female
male

## Supplementary Figure 2.

### Yohimbine-induced changes in NA turnover and gene expression, and validation of opto- and chemogenetic NA release in the hippocampus.

**a**, Quantification of cortical MHPG/NA ratio, as measured by uHPLC, 90 min after systemic injection of vehicle or yohimbine (3 mg/kg, i.p.). Yohimbine increases cortical NA turnover (unpaired *t* test; t(8.9) = –20.099, *p* = 1.015e-08). Vehicle, *n* = 6; Yohimbine, *n* = 7. **b**, Volcano plots showing differentially expressed RNA transcripts between control (C) and acute stress (S) or yohimbine (Yoh) injected animals 45 min after stress or yohimbine injection in the dorsal (dHC) and ventral (vHC) hippocampus, as well as a direct comparison between the two responses. Red and blue values represent changes with FDR-adjusted $p<0.05$ (Veh $n = 5$, Yoh $n = 5$). ****$p < 0.0001$. **c**, Schematic of fiber photometry recording of hippocampal NA during chemogenetic activation of the LC. After 5 min of baseline recording in the homecage animals were injected with clozapine (0.03mg/kg, i.p.) and placed in the OFT for 21min. **d**, Average ΔF/F traces of $GRAB_{NE2m}$ photometry recordings in response to chemogenetic activation of the LC (mean±SEM for hM3DGq+ and hM3DGq-split into females and males, n=3/group/sex). **e**, Peak ΔF/F response of fiber photometry trace. **f**, Schematic of fiber photometry recording of hippocampal NA during optogenetic activation of the LC. Animals were lightly anesthetized (1.5% isoflurane) and recorded in a stereotaxic frame. After 1 min baseline recording, animals were stimulated three times with 5Hz for 10s (10ms pulse width, ~8mW laser power) and recorded for 2 min post-stimulation. **g**, Average ΔF/F traces of the NA sensors $GRAB_{NE1m}$ and nLightG in response to optogenetic activation of the LC (mean±SEM for females and males, n(females)= 10, n(males)=5. **h**, Peak ΔF/F response of fiber photometry traces.

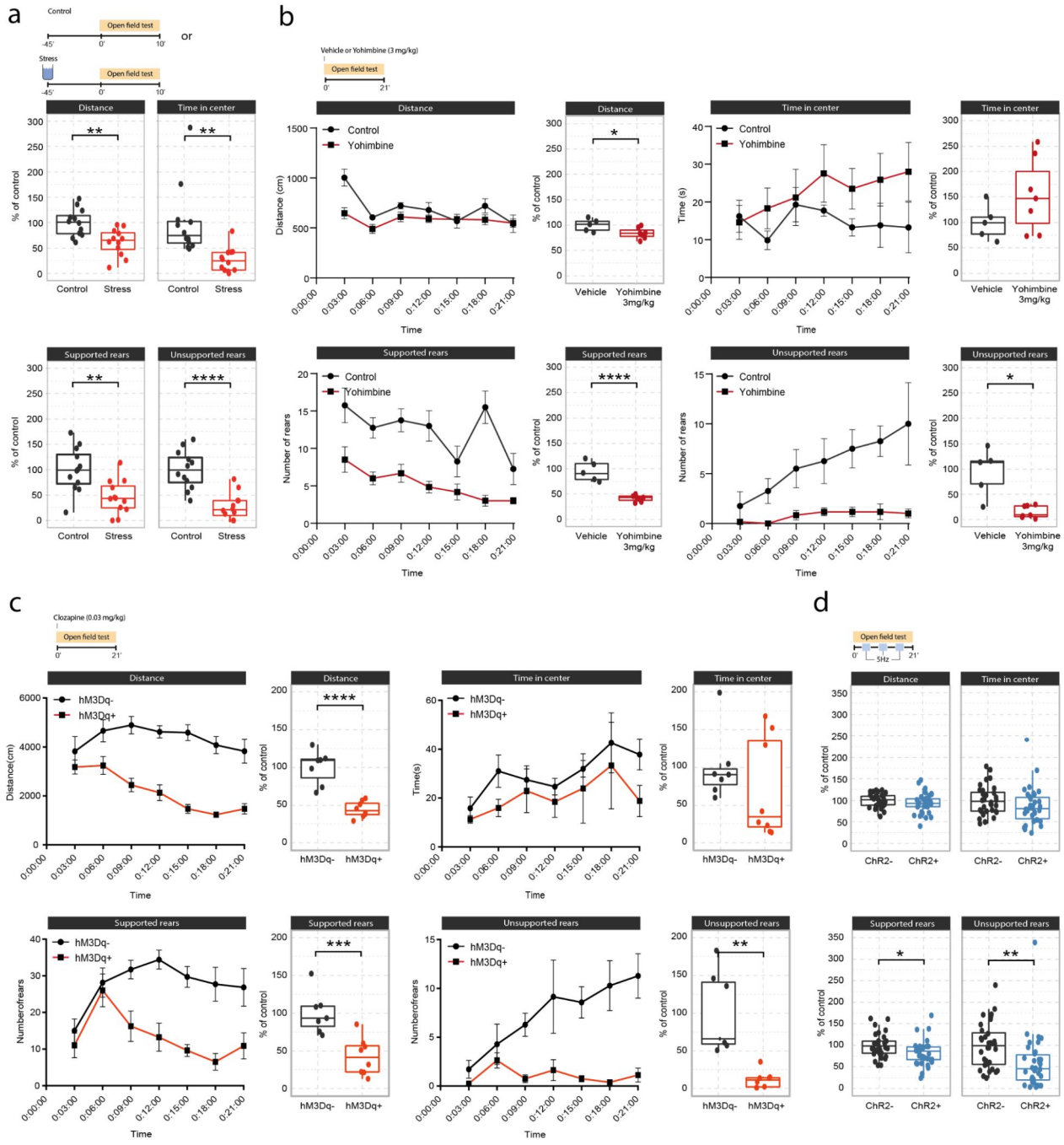
a
Control
Open field test
-45'
0'
10'
or
Stress
Open field test
-45'
0'
10'
Distance
Time in center
% of control
Control
Stress
Supported rears
Unsupported rears
b
Vehicle or Yohimbine (3 mg/kg)
Open field test
0'
21'
Distance
Control
Yohimbine
Distance (cm)
Time
Vehicle
Yohimbine 3mg/kg
Time in center
Time (s)
Supported rears
Number of rears
Unsupported rears
c
Clozapine (0.03 mg/kg)
Open field test
0'
21'
hM3Dq-
hM3Dq+
Distance(cm)
Time(s)
Numberofrears
d
Open field test
0'
5Hz
21'
ChR2-
ChR2+

**Supplementary Figure 3.**

**Effects of acute stress and noradrenergic stimulation on anxiety-like behavior in the open field test.**

**a**, Stress-induced changes in the open field test 45 min after stress onset. Stressed animals show overall reductions in distance traveled (unpaired t-test; t=3.55, df=22, $p$=0.0018), time in center (welch unpaired t-test; t=3.50, df=13.61, $p$=0.0036), supported rears (unpaired t-test; t=3.39, df=22, $p$=0.0026) and unsupported rears (unpaired t-test; t=5.53, df=22, $p$ = 1.47e-05) compared to controls (Control $n$ = 12; Stress $n$ = 12). This data have been previously published (von Ziegler et al. 2022). **b**, Yohimbine (3 mg/kg, i.p.) injected animals show reduced distance traveled (unpaired t-test; t=2.39, df=10, $p$=0.03772), reduced supported rears (unpaired t-test; t=6.56, df=10, $p$=0.00006) and reduced unsupported rears (welch unpaired t-test; t=3.69, df=4.4, $p$ = 0.01785) compared to vehicle injected animals (Vehicle $n$ = 6; Yohimbine $n$ = 7). **c**, Chemogenetic LC activation induced changes in the open field test immediately after clozapine (0.03 mg/kg, i.p.) injection. hM3Dq+ animals show reduced distance traveled (unpaired t-test; t=6.28, df=13, $p$=0.00003), reduced supported rears (unpaired t-test; t=4.28, df=13, $p$=0.0009), as well as reduced unsupported rears (welch unpaired t-test; t=4.28, df=13, $p$ = 0.00437) compared to hM3D-animals (hM3Dq- $n$ = 7; hM3Dq+ $n$ = 8). **d**, Optogenetic 5 Hz LC activation induced changes during the open field test. ChR2+ animals show reduced supported rears (unpaired t-test; t=2.42, df=64, $p$=0.0185) and reduced unsupported rears (unpaired t-test; t=2.91, df=64, $p$ = 0.00499) compared to ChR2-animals (ChR2-$n$ = 32; ChR2+ $n$ = 36). Data expressed as mean ± SEM. *$p$ < 0.05, **$p$ < 0.01, ***$p$ < 0.001, ****$p$ < 0.0001.

**Supplementary Table 1. List of reproducible gene expression changes across various manipulations of the LC-NA system.**

This table displays the logarithmic cumulative rank of genes across all experiments from **figures 1** and **2** in terms of their responsiveness to manipulatios of the LC-NA system. A lower cumulative rank indicates that a gene is among the more significant hits across all analyses (for full list of included analyses see methods). The top 10 genes from this list are shown in **Figure 2o**.

## Supplementary Table 2. Sex-specific regulation of transcription in the ventral hippocampus after swim stress exposure.

Differential expression analysis results for a sex:stress interaction performed across the meta-analysis of vHC datasets 45min after stress initiation (total of 50 males and 20 females). The table merges the results of both the edgeR and the DESeq2 analyses. Detailed information is provided in the sheet "ColumnDefinitions".

# Methods

## Animals

All experiments were conducted in accordance with the Swiss federal guidelines for the use of animals in research and under licenses ZH161/17, ZH106/20 and ZH067/2022 approved by the Zurich Cantonal veterinary office. For experiments with wild type animals, 2-3 month old C57Bl/6J mice were obtained directly from Janvier (France). For experiments involving chemo- and optogenetic LC manipulations, heterozygous C57BL/6-Tg(Dbh-icre)1Gsc mice were kept in breeding

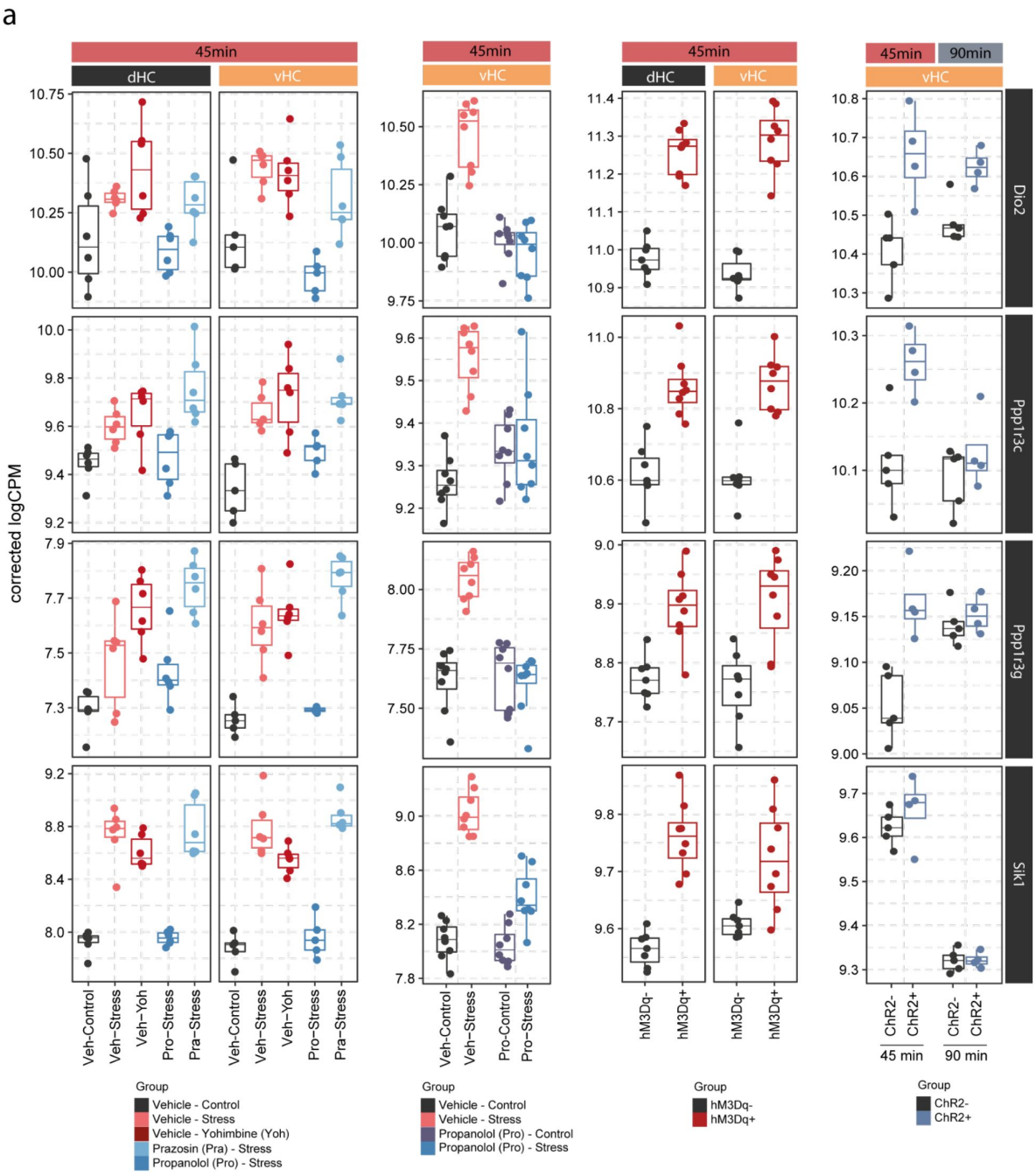


## Supplementary Figure 4.

**Expression of *Dio2*, *Ppp1r3c*, *Ppp1r3g* and *Sik1* is consistent across pharmacological, chemogenetic and optogenetic manipulations of the noradrenergic system.**

**a**, Selective boxplots showing the expression changes of top 4 most responsive genes across all LC-NA manipulations. *Dio2, Ppp1r3c, Ppp1r3g and Sik1* are plotted across experiments in response to acute swim stress exposure, yohimbine (3 mg/kg, i.p.), swim stress and propranolol (10 mg/kg, i.p.), swim stress and prazosin (1 mg/kg, i.p.), as well as chemogenetic and optogenetic LC activation.

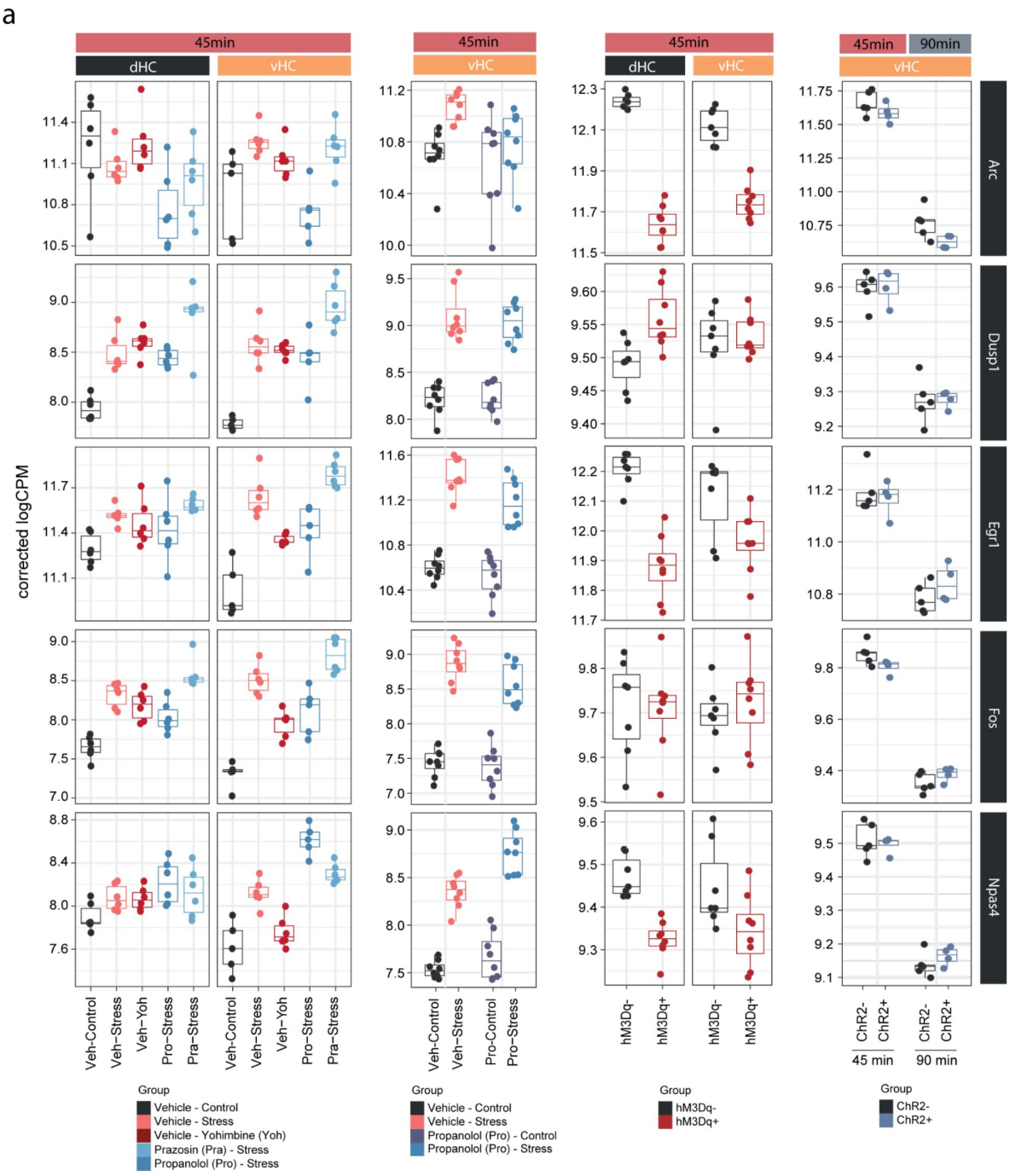


## Supplementary Figure 5.

Neuronal immediate early genes in the hippocampus are not regulated by noradrenaline signaling. **a**, Selective boxplots showing the expression changes of genes associated with neuronal activation (*Arc, Dusp1, Egr1, Fos* and *Npas4*) across experiments in response to acute stress and noradrenergic manipulation. Propranolol was not able to block the stress-induced expression of these genes, and locus coeruleus stimulation was not able to mimic their stress-induced upregulation.

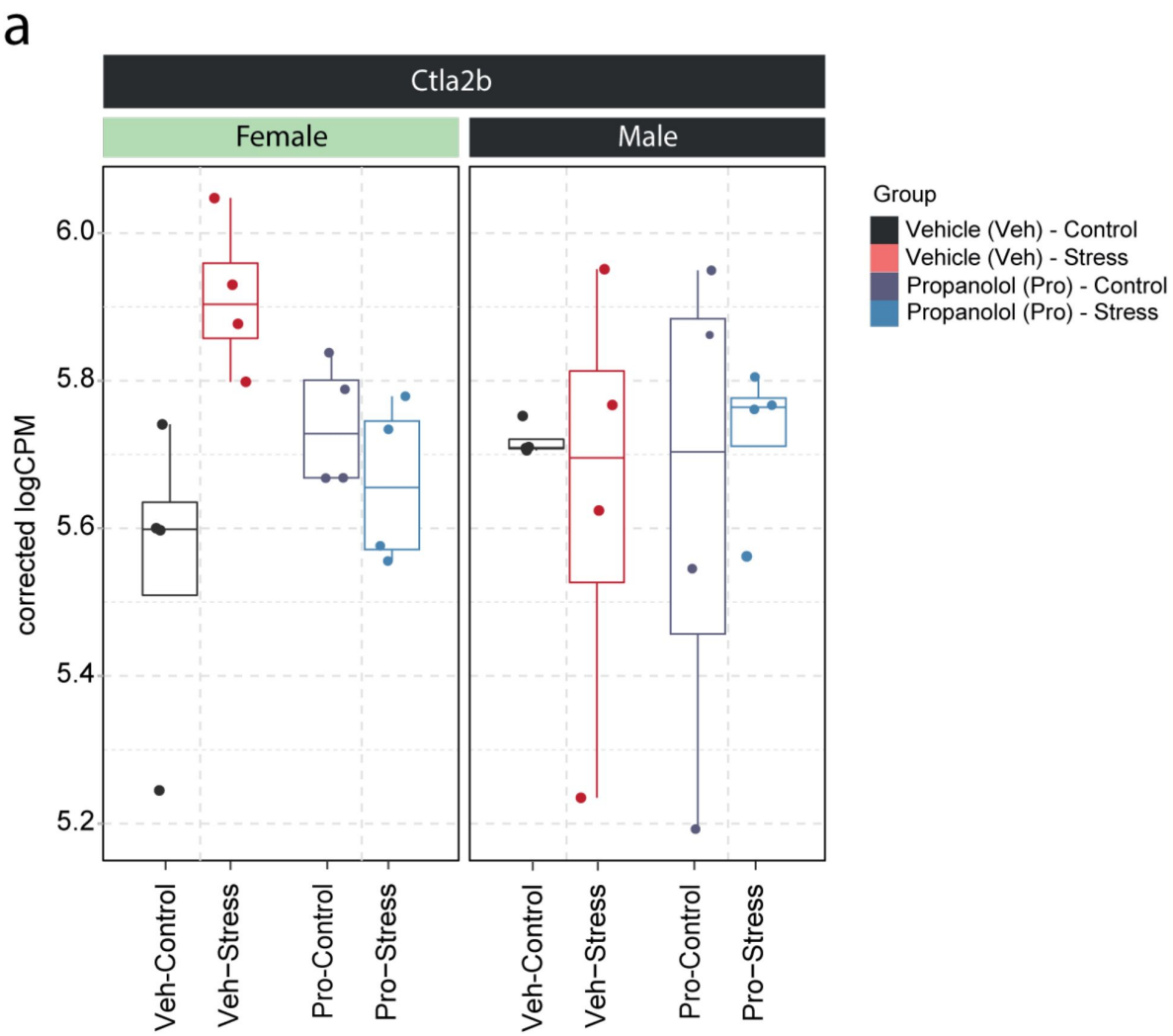


## Supplementary Figure 6.

**Sex dependent expression of Ctla2b in the ventral hippocampus of female and male mice.**

**a**, Selective boxplot of *Ctla2b* expression - from data shown in **figure 1g-h** - in response to acute swim stress and propranolol 45 min after stress onset in female and male mice. *n* = 4 per group.

trios with wild-type C57BL/6J mice at the ETH Zurich animal facility (EPIC). All mice were housed in groups of 2-5 per cage in a temperature- and humidity-controlled facility on a 12-hour reversed light-dark cycle (lights off: 9:15 am; lights on: 9:15 pm), with food and water *ad libitum*, and used for experiments at the age of 2-4 months. All experiments were conducted during the animals' active (dark) phase. For all experiments, mice were single-housed 24 hours before exposure to stress or LC activation, which reduces corticosterone levels in both sexes, and avoids confounding gene expression effects from social stressors (Roszkowski et al. 2016; Bohacek et al. 2015).

## Stereotactic Surgeries

For experiments involving hippocampal infusions, female C57BL/6-Tg(Dbh-icre)1Gsc mice at the age of 2-3 months were subjected to stereotactic surgery. The mice were anesthetized with 4% isoflurane and then placed in a stereotaxic frame with continuous anesthesia of 2% isoflurane. For analgesia, animals received a subcutaneous injection of 5 mg/kg Meloxicam and buprenorphine (0.1 mg/kg), as well as application of the local analgesics lidocaine (2 mg/kg) and bupivacaine (2 mg/kg) before and after surgery. After the skull was exposed, bregma (defined as the intersection of the coronal and sagittal suture) was located and the skull placement corrected for tilt and scaling. Bilateral holes were drilled above the hippocampus at −1.8 mm AP and +/- 1.5 mm ML from bregma, followed by the implantation of a bilateral guide cannula (62036, RWD Life Science, China) into the hippocampus (coordinates from bregma: −1.8 mm AP, +/- 1.5 mm ML, - 1.5 mm DV).

For chemo- and optogenetic experiments male C57BL/6-Tg(Dbh-icre)1Gsc mice at the age of 2-3 months were subjected to stereotactic surgery. The mice were anesthetized with 4% isoflurane and then placed in a stereotaxic frame with continuous anesthesia of 2% isoflurane. For analgesia, animals received a subcutaneous injection of 5 mg/kg Meloxicam and a local anesthetic (Emla cream; 5% lidocaine, 5% prilocaine) before and after surgery. After the skull was exposed, bregma was located and the skull placement corrected for tilt and scaling. Bilateral (chemogenetics) or unilateral (Right hemisphere, optogenetics) small holes were drilled above the LC at −5.4 mm AP and 0.9 mm ML from bregma. A pneumatic injector (Narishige, IM-11-2) and calibrated microcapillaries (Sigma-Aldrich, P0549) were then used to inject 1 µL of virus to the LC (coordinates from bregma: −5.4 mm AP, ± 1.0 mm ML, −3.8 mm DV). All Viral vectors were obtained from the Viral Vector Facility (VVF) of the Neuroscience Center Zurich. For chemogenetic experiments, either ssAAV-5/2-hSyn1-dlox-hM3D(Gq)_mCherry(rev)-dlox-WPRE-hGHp(A) (hM3Dq+) or ssAAV-5/2-hSyn1-dlox-mCherry(rev)-dlox-WPRE-hGHp(A) (hM3Dq-) were injected bilaterally for all experiments except fiber photometry recordings where animals were injected unilaterally.

For optogenetic experiments, ssAAV-5/2-hEF1α-dlox-hChR2(H134R)_EYFP(rev)-dlox-WPRE-hGHp(A) (ChR2+) or ssAAV-5/2-hEF1a-dloxEGFP(rev)-dlox-WPRE-bGHp(A) (ChR2-) were delivered unilaterally to the right hemisphere locus coeruleus. For retrograde activation of hippocampus projecting LC neurons, animals received one injection of either ssAAV-retro/2-hEF1a-dlox-hChR2(H134R)_EYFP(rev)-dlox-WPRE-hGHp(A) (ChR2+) or ssAAV-retro/2-hEF1a-dlox-mCherry(rev)-dlox-WPRE-hGHp(A) (ChR2-) to the ipsilateral dHC (coordinates from bregma: −2.10 mm AP, 1.5 mm ML; −1.8 mm DV) and vHC (coordinates from bregma: −3.30 mm AP, 2.75 mm ML; −4.0 mm DV). Additionally, all optogenetic animals were unilaterally implanted with an optic fiber (200 µm diameter, 0.22 NA) above the LC (coordinates from bregma: −5.4 mm AP, 0.9 mm ML, −3.5 mm DV). For fiber photometry recordings, animals were injected with the optogenetic actuator ChrimsonR (ssAAV-5/2-hEF1α/hTLV1-dlox-ChrimsonR_ tdTomato(rev)-dlox-WPRE-bGHp(A); 4.7×10E12 vg/ml). Additionally, animals for both optogenetic and chemogenetic fiber photometry recordings received a second injection of a genetically encoded NA sensor (ssAAV-9/2-hSyn1-GRAB(NE1m)-WPRE-hGHp(A); 5.5×10E12 vg/ml, ssAAV-9/2-hSyn1-chI-nLightG-WPRE-bGHp(A); 5.5×10E12, or ssAAV-9/2-hSyn1-GRAB(NE2m)-WPRE-hGHp(A); 0.5×10E12 vg/ml) into the ipsilateral vHC (coordinates: AP −3.2 mm, ML −3.3 mm, DV −3.8 mm). To record from the vHC, an optic fiber was implanted 200 µm above the injection site (200 µm, NA=0.37; Neurophotometrics, USA). The health of all animals was monitored over the course of 3 consecutive days post-surgery. Experiments on

operated animals were conducted 4-8 weeks post-surgery to allow for recovery and sufficient virus expression. All viruses were obtained from the Viral Vector Facility of the University of Zurich and ETH Zurich.

## Drug injections/infusions

All drugs were freshly prepared immediately before experiments and dissolved in phosphate-buffered 0.9% saline (Gibco, pH 7.4). Drugs were administered intraperitoneally at their corresponding dosages: Yohimbine-Hydrochloride (3 mg/kg, Merck, Germany), Propranolol-Hydrochloride (10 mg/kg, Merck, Germany), Prazosin-Hydrochloride (1 mg/kg, Merck, Germany) and Clozapine (0.03mg/kg, Merck, Germany).

For intra-hippocampal infusions of isoproterenol hydrochloride (Merck, Germany), animals were restrained and the guide cannula was inserted with an injector needle (62236, RWD Life Science, China) connected to an infusion pump (R462 Syringe Pump, RWD Life Science, China) via plastic tubing. Prior to attachment, the tubing was filled with sunflower seed oil (Merck, Germany) and vehicle (0.9% saline) or isoproterenol, separated by a small air bubble. Afterwards, animals were allowed to freely roam their home cage for 2 minutes followed by bilateral intra-hippocampal infusions of vehicle drug or 1 µl of isoproterenol (3 µg/µl diluted in phosphate-buffered 0.9% saline) at 50 µl/min. Diffusion of vehicle and isoproterenol was allowed for another 2 min, before the animal was detached from the infusion setup and returned to its homecage.

## Fiber photometry

Fiber photometry recordings were performed as previously reported (Grimm et al. 2022). In short, the green fluorescence signal from the NA sensors $GRAB_{NE1m}$, $GRAB_{NE2m}$, or nLightG were recorded using a commercially available photometry system (Neurophotometrics, Model FP3002) controlled via the open-source software Bonsai (2.6.2 version). Two LEDs were used to deliver interleaved excitation light: a 470 nm LED for recording NA-dependent fluorescent signal ($F^{470}$) and a 415 nm LED for NA – independent control signals ($F^{415}$). Recording rate was set at 60 Hz for both LEDs allowing 30 Hz per channel. Excitation power at the fiber tip (200 µm, 0.39 numerical aperture; Doric Lenses) was set to 25-35 µW. Recordings during optogenetic LC stimulation were performed during light anesthesia (1.5% isoflurane) while chemogenetic LC activation was recorded in awake, well-handled animals.

## Forced swim test

For the forced cold swim stress, mice were placed for 6 min in a plastic beaker (20 cm diameter, 25 cm deep) filled with 18 ± 0.1°C water to 17 cm, in a room with dim red lighting. Immediately after stress exposure, mice returned to their assigned single-housing homecage.

## Open field test (OFT)

Open-field testing was performed in a square 45 cm (l) × 45 cm (w) × 40 cm (h) arena, and consisted of four black Plexiglas walls and a white PVC floor. Mice were tested under dim lighting (5 lux at the center of the arena). Mice were placed directly into the center of the open field and the tracking/recording was initiated 2 seconds after the mouse was detected. The test lasted 10 min for acute stress exposed animals, 21 min for yohimbine and optogenetic stimulated animals and 30 min for chemogenetic stimulated animals. Distance, time in center, supported and unsupported rearings were tracked by the software EthoVision XT14 (Noldus, Netherlands) and manual scoring. For pharmacological and chemogenetic experiments, animals received an i.p injection of yohimbine (3 mg/kg) or clozapine (0.03 mg/kg) immediately before being placed into the arena. For optogenetic experiments, animals were attached to the optic fiber and directly placed into the arena.

## Optogenetic stimulation

Across optogenetic experiments the LC was stimulated with either 473 nm or 635 nm light at 10 mW power and 3 Hz, 5 Hz or 15 Hz frequency (10 ms pulse width) alternating between 3 min off and on as previously described (McCall et al. 2015; Grimm et al. 2022).

## Pupillometry

Pupillometry was used to evaluate optogenetic LC stimulation as previously described (Privitera et al. 2020). At 3-4 weeks post-surgery, ChR2- and ChR2+ animals were anesthetized with 4% isoflurane and then placed in a stereotaxic frame with continuous anesthesia of 2% isoflurane. Recordings were performed of the right eye ipsilateral to the stimulated LC and consisted of an initial baseline recording of 60 seconds, followed by tonic LC stimulation (5 Hz at 10 mW for 10 s) and 1 min post stimulation recording. Pupil videos were tracked with DeepLabCut and analyzed with the Pupillometry App.

## Tissue collection

At the appropriate time point after initiation of stress (for immediate groups within maximum 1 min after offset of stress) or LC activation, mice were euthanized by cervical dislocation and decapitation. The brain was quickly dissected on a cold glass plate and isolated hippocampi were separated by a cut at a ratio of 1:2 to divide the dHC and vHC. For experiments that were analyzed with uHPLC additionally the whole cortex was also collected. Isolated tissues were then snap-frozen in liquid nitrogen and stored at −80°C until further processing. For immunohistochemistry, the hindbrain (containing the LC) was isolated with a single cut from a razor blade at the beginning of the cerebellum and directly transferred to a tube with 4% paraformaldehyde solution. All tissue dissections were performed between 11am and 5pm during the dark phase of the 12-hour reversed light-dark cycle.

## Immunohistochemistry

LC containing hindbrain samples were fixed for 2 hours in ice-cold paraformaldehyde solution (4% PFA in PBS, pH 7.4). The tissue then was rinsed with PBS and stored in a sucrose solution (30% sucrose in PBS) at 4°C, overnight. The tissue was frozen in tissue mounting medium (Tissue-Tek O.C.T Compound, Sakura Finetek Europe B.V., Netherlands), and sectioned coronally using a cryostat (Leica CM3050 S, Leica Biosystems Nussloch GmbH) into 40 µm thick sections. The sections were immediately transferred into ice-cold PBS. LC containing sections were stained in primary antibody solution with 0.05% Triton X-100, and 4% normal goat serum in PBS at 4C under continuous agitation over 2 nights. The primary antibodies used were: mouse anti-TH (22941, Immunostar, 1:1000), chicken anti-GFP (ab13970, Abcam, 1:1000) and rabbit anti-cFOS (226 003, Synaptic Systems, 1:5000). Afterwards, the sections were washed 3 times in PBS, and transferred to secondary antibody solution containing 0.05% Triton X-100, and 4% normal goat serum in PBS. The secondary antibodies used were: goat anti-mouse Alexa 488 (ab150113, Abcam, 1:300), goat anti-mouse Cy3 (115-165-003, Jackson ImmunoResearch, 1:300), goat anti-chicken Alexa 488 (A-11039, Thermo Fischer Scientific, 1:300), goat anti-rabbit Alexa 488 (A-11008 Thermo Fisher Scientific, 1:500), goat anti-rabbit Alexa 546 (A-11035, Thermo Fisher Scientific, 1:300) and donkey anti-mouse Alexa 647 (A-31571, Thermo Fisher Scientific, 1:300). Nissl was stained by NeuroTrace 640/660 Nissl stain (N21483, Thermo Fisher Scientific). After 3 more PBS washes, the sections were mounted onto glass slides (Menzel-Glaser SUPERFROST PLUS, Thermo Scientific), air-dried and coverslipped with Dako fluorescence mounting medium (Agilent Technologies). Microscopy images were acquired in a confocal laser-scanning microscope (CLSM 880, Carl Zeiss AG, Germany) with a 20x objective. Images were analyzed using FIJI and for cFos quantification TH+ and cFos+ cells were counted manually.

## Ultra-high performance liquid chromatography (uHPLC)

To quantify noradrenergic (NA; MHPG) compounds from cortical and hippocampal tissue, a reversed-phase uHPLC system coupled with electrochemical detection (RP-uHPLC-ECD) was used (Alexys$^{TM}$ Neurotransmitter Analyzer, Antec Leyden, Zoeterwoude, Netherlands). In short, our previously validated RP-HPLC method with ion pairing chromatography was applied as described (Van Dam et al., 2014), albeit with minor modifications regarding the installed column (BEH C18 Waters column, 150 mm x 1 mm, 1.7 µm particle size) and pump preference (LC110S pump, 470-480 bar; flow rate of 62 L/min), achieving the most optimal separation conditions in a RP-UHPLC setting. Brain samples were defrosted to 4°C and subsequently homogenized in 800-900 µL ice-cold sample buffer (50 mM citric acid, 50 mM phosphoric acid, 0.1 mM EDTA, 8 mM KCl and 1.8 mM octane-1-sulfonic acid sodium salt (OSA), adjusted to pH = 3.6), using a Precellys® Minilys Personal Tissue Homogenizer (Bertin Technologies$^{TM}$, France) with CK14 1.4 mm ceramic beads (40-60 sec approximately, full speed). To remove excess proteins, 450 mL homogenate was transferred onto a 10,000 Da Amicon Ultra 0.5 Centrifugal Filter (Millipore, Ireland) that had been pre-washed twice using 450 µL sample buffer (centrifugation: 14,000 x g, 20 min, 4°C). The Amicon filter loaded with the homogenate was then centrifuged (14,000 x g, 20 min, 4°C). Finally, the filtrate was transferred into a polypropylene vial (0.3 mL, Machery-Nagel GmbH & Co. KG, Germany) and automatically injected into the uHPLC column by the Alexys AS110 Autosampler (5 µL sample loop). Levels of the monoamines and metabolites were calculated using Clarity software$^{TM}$ (DataApex Ltd., v86.12.0.77208, 2015, Prague, Czech Republic).

## RNA extraction

Dorsal and ventral hippocampal samples were homogenized in 500 µL Trizol (Invitrogen 15596026) in a tissue lyser bead mill (Qiagen, Germany) at 4°C for 2 mins, and RNA was extracted according to manufacturer's recommendations. This was followed by determining RNA purity and quantity with a UV/V spectrophotometer (Nanodrop 1000).

## Bulk RNA sequencing and data analysis

For experiments shown in **Figure 1c-e** and **2**, bulk mRNA sequencing was performed at the Functional Genomics Center Zurich (FGCZ) core facility. Data shown in **figure 1c-e** and **2c-d** belong to the same experiment and were split up for better visualization of effects after sample processing and RNA sequencing analysis was performed. RNA integrity was assessed with high sensitivity RNA screen tape on an Agilent Tape Station/Bioanalyzer, according to the manufacturer's protocol. The RIN values of all samples ranged from 8.4 to 10.0. For library preparation, the TruSeq stranded RNA kit (Illumina Inc.) was used according to the manufacturer's protocol. For bulk sequencing library preparation, the TruSeq stranded RNA kit (Illumina Inc.) was used according to the manufacturer's protocol. The mRNA was purified by polyA selection, chemically fragmented and transcribed into cDNA before adapter ligation. Single-end (100nt) sequencing was performed with HiSeq 4000. Samples within experiments were each run on one or multiple lanes and demultiplexed. A sequencing depth of ~20M reads per sample was used. Bulk mRNA sequencing for experiments shown in **Figure 1g-h** and **3** were performed at Novogene UK. Total RNA samples were used for library preparation using NEB Next® Ultra RNA Library Prep Kit for Illumina®. Indices were included to multiplex multiple samples. Briefly, mRNA was purified from total RNA using poly-T oligo-attached magnetic beads. After fragmentation, the first strand cDNA was synthesized using random hexamer primers followed by the second strand cDNA synthesis. The library was ready after end repair, A-tailing, adapter ligation, and size selection. After amplification and purification, insert size of the library was validated on an Agilent 2100 and quantified using quantitative PCR (Q-PCR). Libraries were then sequenced on Illumina NovaSeq 6000 S4 flowcell with PE150 according to results from library quality control and expected data volume. Samples within experiments were each run on one or multiple lanes and demultiplexed. A sequencing depth of ~40M reads per sample was used.

For all experiments, adapters were trimmed using cutadapt (Martin 2011) with a maximum error rate of 0.05 and a minimum length of 15. Kallisto (v0.44.0) (Bray et al. 2016) was used for pseudo alignment of reads on the transcriptome level using the genecode.vM17 assembly with 30 bootstrap samples and an estimated fragment length of 200 ± 20 for single-end samples. For differential gene expression (DGE) analysis we aggregated reads of protein coding transcripts and used R (v. 4.0.3) with the package "edgeR" (v 3.32.1) for analysis. A filter was used to remove genes with low expression prior to DGE analysis. EdgeR was then used to calculate the normalization factors (TMM method) and estimate the dispersion (by weighted likelihood empirical Bayes). For two group comparisons the genewise exact test was used, for more complex designs we used a generalized linear model (GLM) with empirical Bayes quasi-likelihood F-tests. Exact specifications for each tested model can be found under *https://github.com/ETHZ-INS/LC_Opto_Transcriptomics*. For multiple testing correction the Benjamini-Hochberg false discovery rate (FDR) method was used, and for interaction terms (e.g. stress:sex or stress:injection), FDR was calculated only on the genes that have a significant stress effect. For analyses of data-sets originating from multiple experiments we further employed SVA correction to correct for processing specific effects (Leek et al. 2012). Surrogate variables independent of experimental groups were identified using the SVA package (v3.38.0) on data after DESeq2 (v1.30.1) variance-stabilization (Love, Huber, and Anders 2014), and were then included as additive terms in the GLMs. Heatmaps were produced with the sechm (v1.5.1) package. To avoid rare extreme values from driving the scale, the color scale is linear for values within a 98% interval, and ordinal for values outside it. Unless otherwise specified, the rows were sorted using the features' angle on a two-dimensional projection of the plotted values, as default in sechm.

For the combined analysis of consistent effects across yohimbine injection, chemogenetic and optogenetic stimulation we first combined all three datasets and modeled batch effects using SVA correction. We then designed a combined response variable that was set to control (homecage in the injection experiment, hM3Dq- in chemogenetic and ChR2- in optogenetic) or response (yohimbine in the injection experiment, hM3Dq+ in chemogenetic and ChR2+ in optogenetic). We then fit an additive generalized linear model with the newly defined response variable and the surrogate variables from the SVA correction and tested it for the response variable coefficient.

For the cumulative rank analysis, statistical results were used from multiple analyses (Stress group vs propranolol group in vHC of the first injection experiment; Stress group vs propranolol group in dHC of the first injection experiment; Stress:Propranolol interaction in second injection experiment; effect of chemogenetic LC activation in vHC; effect of chemogenetic LC activation in dHC; effect of optogenetic LC activation after 45 minutes). Then, in each analysis the gene with the lowest p-value was set to rank 1, the one with the highest to rank N. These ranks were then summed up across all analyses to generate the cumulative rank.

## Reverse transcription quantitative real-time polymerase chain reaction (RT-qPCR)

Reactions were conducted using SYBR green (Roche) on a CFX384 Touch Real-Time PCR Detection System (Bio-Rad) and normalized against Tubulin delta 1 (Tubd1). Cycling conditions were 5 min at 95 °C, then 50 cycles with denaturation (10 s at 95 °C), annealing (10 s at 60 °C), and elongation (10 s at 72 °C). Primers were designed using PrimerBlast (Kozyreva et al. 2021) and tested for quality and specificity by melt-curve analysis, gel electrophoresis and appropriate negative controls. Forward (FP) and reverse (RP) primer sequences were as follows:

| | |
|---|---|
| Tubd1: | FP: TCTCTTGCTAACTTGGTGGTCCTC / RP: GCTGGGTCTTTAAATCCCTCTACG |
| Apold1: | FP: ACCTCAGGCTCTCCTTCCATCATC / RP: ACCCGAGACAAAGCACCAATGC |
| Dio2: | FP: GCCTACAAACAGGTTAAACTGGGTG / RP: CCATCAGCGGTCTTCTCC |
| Sik1: | FP: ACAGCTCACTTCAGCCCTTAT / RP: CTCGCTGATAGCTGTGTCCA |
| Ppp1r3c: | FP: TGAGCTGCACCAGAATGATCC / RP:GGTGGTGAATGAGCCAAGCA |

### Statistics

We used a block design for experiments. Animals and samples were split into multiple blocks, containing one replicate of each condition. Experimental and processing order within these blocks was randomized. Investigators were blinded during behavior and sample processing, but not during the analysis process. However, the same algorithmic analysis methods were used for all samples within each sequencing experiment. Analysis was performed in R or GraphPad Prism 9.2.0. For statistical analyses of behavior, pupillometry, immunohistochemistry and uHPLC data, we used independent samples t tests when comparing two independent groups. When comparing more than two groups we used one-way ANOVAs if there was a single independent variable, or two-way ANOVAs for two-factorial designs (e.g., injection x group). Significant main effects and interactions were analyzed using Tukey's post hoc tests. For linear model analysis we used the function lm() from the "stats" package in R and F-statistics for significance testing. No statistical method was used to predetermine sample size. No data were excluded from the analyses.

## Data availability

The sequencing data data generated in this study has been deposited in the Gene Expression Omnibus database under accession code GSE218315 (reviewer token yhilwoocbhujjwp) for all injection experiments and GSE218313 for chemo and optogenetic experiments (reviewer token stoxiksgfhmpjiz).

## Code availability

Code for all analyses (independent scripts) presented here is available on GitHub under *https://github.com/ETHZ-INS/Privitera-et.-al.-2023*.

## Acknowledgements

The lab of JB was supported by the ETH Zurich, ETH Project Grant ETH-20 19-1, the Swiss National Science Foundation (grants 310030_172889/1 and 310030_204372), the Botnar Research Centre for Child Health, the Swiss 3R Competence Center, Roche, the Hochschulmedizin Zürich Flagship project STRESS, the Forschungskredit of the University of Zurich, the Novartis Foundation for Medical-Biological Research, the Swiss Foundation for Excellence and Talent in Biomedical Research, the Vontobel Foundation, the Betty and David Koetser Foundation for Brain Research. The lab of PPDD and DVD was supported by the University of Antwerp, Research Foundation Flanders (FWO), Joint Programming Initiative Neurodegenerative Diseases (JPND) and ZonMW (HEROES 73305172), Alzheimer Nederland and Neurosearch Antwerp. We thank the staff of the EPIC for the excellent animal care and their service to our animal facility and Prof. Isabelle Mansuy for providing support and space. We thank Han-Yu Lin and Justine Leonardi for help with sample processing and Julia Bode for maintaining the animal colony.

# References


Allaman I., Pellerin L., Magistretti P. J. (2000) **Protein Targeting to Glycogen mRNA Expression Is Stimulated by Noradrenaline in Mouse Cortical Astrocytes** *Glia* **30**:382–91

Bangasser Debra A., Eck Samantha R., Sanchez Evelyn Ordoñes (2019) **Sex Differences in Stress Reactivity in Arousal and Attention Systems** *Neuropsychopharmacology: Official Publication of the American College of Neuropsychopharmacology* **44**:129–39

Benito Eva, Barco Angel (2015) **The Neuronal Activity-Driven Transcriptome** *Molecular Neurobiology* **51**:1071–88

Bertorello Alejandro Mario, Zhu Jian-Kang (2009) **SIK1/SOS2 Networks: Decoding Sodium Signals via Calcium-Responsive Protein Kinase Pathways** *Pflugers Archiv: European Journal of Physiology* **458**:613–19

Bianco Antonio C., Dumitrescu Alexandra, Gereben Balázs, Ribeiro Miriam O., Fonseca Tatiana L., Fernandes Gustavo W., Bocco Barbara M. L. C. (2019) **Paradigms of Dynamic Control of Thyroid Hormone Signaling** *Endocrine Reviews* **40**:1000–1047

Bohacek Johannes, Manuella Francesca, Roszkowski Martin, Mansuy Isabelle M. (2015) **Hippocampal Gene Expression Induced by Cold Swim Stress Depends on Sex and Handling** *Psychoneuroendocrinology* **52**:1–12

Bohmbach Kirsten, Masala Nicola, Schönhense Eva M., Hill Katharina, Haubrich André N., Zimmer Andreas, Opitz Thoralf, Beck Heinz, Henneberger Christian (2022) **An Astrocytic Signaling Loop for Frequency-Dependent Control of Dendritic Integration and Spatial Learning** *Nature Communications* **13**

Bouret Sebastien, Sara Susan J. (2002) **Locus Coeruleus Activation Modulates Firing Rate and Temporal Organization of Odour-Induced Single-Cell Responses in Rat Piriform Cortex** *The European Journal of Neuroscience* **16**:2371–82

Bray Nicolas L., Pimentel Harold, Melsted Páll, Pachter Lior (2016) **Near-Optimal Probabilistic RNA-Seq Quantification** *Nature Biotechnology* **34**:525–27

Campos-Barros A., Meinhold H., Stula M., Müller F., Köhler R., Eravci M., Putzien O., Baumgartner A. (1994) **The Influence of Desipramine on Thyroid Hormone Metabolism in Rat Brain** *The Journal of Pharmacology and Experimental Therapeutics* **268**:1143–52

Cembrowski Mark S., Bachman Julia L., Wang Lihua, Sugino Ken, Shields Brenda C., Spruston Nelson (2016) **Spatial Gene-Expression Gradients Underlie Prominent Heterogeneity of CA1 Pyramidal Neurons** *Neuron* **89**:351–68

Coggan Jay S., Keller Daniel, Calì Corrado, Lehväslaiho Heikki, Markram Henry, Schürmann Felix, Magistretti Pierre J. (2018) **Norepinephrine Stimulates Glycogenolysis in Astrocytes to Fuel Neurons with Lactate** *PLoS Computational Biology* **14**

Dienel Gerald A (2017) **The Metabolic Trinity, Glucose-Glycogen-Lactate, Links Astrocytes and Neurons in Brain Energetics, Signaling, Memory, and Gene Expression** *Neuroscience Letters* **637**:18–25

Endo Fumito, Kasai Atsushi, Soto Joselyn S., Yu Xinzhu, Qu Zhe, Hashimoto Hitoshi, Gradinaru Viviana, Kawaguchi Riki, Khakh Baljit S. (2022) **Molecular Basis of Astrocyte Diversity and Morphology across the CNS in Health and Disease** *Science* https://doi.org/10.1126/science.adc9020

Feldman J. D., Vician L., Crispino M., Hoe W., Baudry M., Herschman H. R. (2000) **The Salt-Inducible Kinase, SIK, Is Induced by Depolarization in Brain** *Journal of Neurochemistry* **74**:2227–38

Feng Jiesi, Zhang Changmei, Lischinsky Julieta E., Jing Miao, Zhou Jingheng, Wang Huan, Zhang Yajun, et al. (2019) **A Genetically Encoded Fluorescent Sensor for Rapid and Specific In Vivo Detection of Norepinephrine** *Neuron* **102**:745–61

Fernandez-Albert J., Lipinski M., Lopez-Cascales M. T., Rowley M. J., Martin-Gonzalez A. M., Del Blanco B., Corces V. G., Barco A. (2019) **Immediate and Deferred Epigenomic Signatures of in Vivo Neuronal Activation in Mouse Hippocampus** *Nature Neuroscience* **22** https://doi.org/10.1038/s41593-019-0476-2

Fink George (2016) **Stress: Neuroendocrinology and Neurobiology: Handbook of Stress Series**

Floriou-Servou Amalia, von Ziegler Lukas M., Waag Rebecca, Schläppi Christa, Germain Pierre-Luc, Bohacek Johannes (2021) **The Acute Stress Response in the Multiomic Era** *Biological Psychiatry* **89**:1116–26

Floriou-Servou Amalia, von Ziegler Lukas, Stalder Luzia, Sturman Oliver, Privitera Mattia, Rassi Anahita, Cremonesi Alessio, Thöny Beat, Bohacek Johannes (2018) **Distinct Proteomic, Transcriptomic, and Epigenetic Stress Responses in Dorsal and Ventral Hippocampus** *Biological Psychiatry* **84**:531–41

Gao Virginia, Suzuki Akinobu, Magistretti Pierre J., Lengacher Sylvain, Pollonini Gabriella, Steinman Michael Q., Alberini Cristina M. (2016) **Astrocytic β2-Adrenergic Receptors Mediate Hippocampal Long-Term Memory Consolidation** *Proceedings of the National Academy of Sciences of the United States of America* **113**:8526–31

Gerstner Nathalie, Krontira Anthi C., Cruceanu Cristiana, Roeh Simone, Pütz Benno, Sauer Susann, Rex-Haffner Monika, Schmidt Mathias V., Binder Elisabeth B., Knauer-Arloth Janine (2022) **DiffBrainNet: Differential Analyses Add New Insights into the Response to Glucocorticoids at the Level of Genes, Networks and Brain Regions** https://doi.org/10.1101/2022.04.21.489034

Ghosh Abhinaba, Massaeli Faghihe, Power Kyron D., Omoluabi Tamunotonye, Sarah E, Torraville Julia, Pritchett B., Sepahvand Tayebeh, et al. (2021) **Locus Coeruleus Activation Patterns Differentially Modulate Odor Discrimination Learning and Odor Valence in Rats** *Cerebral Cortex Communications* **2**

Gibbs Marie E., Hutchinson Dana, Hertz Leif (2008) **Astrocytic Involvement in Learning and Memory Consolidation** *Neuroscience and Biobehavioral Reviews* **32**:927–44

Girgenti Matthew J., Pothula Santosh, Newton Samuel S. (2021) **Stress and Its Impact on the Transcriptome** *Biological Psychiatry* **90**:102–8

Gray J. D., Rubin T. G., Hunter R. G., McEwen B. S. (2013) **Hippocampal Gene Expression Changes Underlying Stress Sensitization and Recovery** *Molecular Psychiatry* **19**:1171–78

Grimm Christina, Duss Sian N., Privitera Mattia, Munn Brandon R., Frässle Stefan, Chernysheva Maria, Patriarchi Tommaso, et al. (2022) **Locus Coeruleus Firing Patterns Selectively Modulate Brain Activity and Dynamics** *bioRxiv* https://doi.org/10.1101/2022.08.29.505672

Hansen Niels (2017) **The Longevity of Hippocampus-Dependent Memory Is Orchestrated by the Locus Coeruleus-Noradrenergic System** *Neural Plasticity* **2017**

Harley Carolyn W., Yuan Qi (2021) **Locus Coeruleus Optogenetic Modulation: Lessons Learned from Temporal Patterns** *Brain Sciences* **11** https://doi.org/10.3390/brainsci11121624

Hermans Erno J., Henckens Marloes J. A. G., Joëls Marian, Fernández Guillén (2014) **Dynamic Adaptation of Large-Scale Brain Networks in Response to Acute Stressors** *Trends in Neurosciences* **37**:304–14

Hirschberg Stefan, Li Yong, Randall Andrew, Kremer Eric J., Pickering Anthony E. (2017) **Functional Dichotomy in Spinal-vs Prefrontal-Projecting Locus Coeruleus Modules Splits Descending Noradrenergic Analgesia from Ascending Aversion and Anxiety in Rats** *eLife* **6** https://doi.org/10.7554/eLife.29808

Huang Bing S., White Roselyn A., Leenen Frans H. H. (2012) **"Possible Role of Brain Salt-Inducible Kinase 1 in Responses to Central Sodium in Dahl Rats."** *American Journal of Physiology-Regulatory, Integrative and Comparative Physiology* https://doi.org/10.1152/ajpregu.00381.2011

Iqbal Zafar, Lei Zhuogui, Ramkrishnan Aruna S., Liu Shu, Hasan Mahadi, Akter Mastura, Lam Yuk Yan, Li Ying (2023) **Adrenergic Signalling to Astrocytes in Anterior Cingulate Cortex Contributes to Pain-Related Aversive Memory in Rats** *Communications Biology* **6**

Jaitovich Ariel, Bertorello Alejandro M. (2010) **Intracellular Sodium Sensing: SIK1 Network, Hormone Action and High Blood Pressure** *Biochimica et Biophysica Acta* **1802**:1140–49

Joëls Marian, Baram Tallie Z. (2009) **The Neuro-Symphony of Stress** *Nature Reviews. Neuroscience* **10**:459–66

Johnston A. L., Baldwin H. A., File S. E. (1988) **Measures of Anxiety and Stress in the Rat Following Chronic Treatment with Yohimbine** *Journal of Psychopharmacology* **2**:33–38

Kagiampaki Zacharoula, Rohner Valentin, Kiss Cedric, Curreli Sebastiano, Dieter Alexander, Wilhelm Maria, Harada Masaya, et al. (2023) **Sensitive Multicolor Indicators for Monitoring Norepinephrine in Vivo** *Nature Methods* **20**:1426–36

Kozyreva A. A., Zlotina A. M., Golovkin A. S., Kalinina O. V., Kostareva A. A. (2021) **Primer Designing in Primer-BLAST** *Translational Medicine* https://doi.org/10.18705/2311-4495-2021-8-3-37-52

Leek Jeffrey T., Evan Johnson W., Parker Hilary S., Jaffe Andrew E., Storey John D. (2012) **The Sva Package for Removing Batch Effects and Other Unwanted Variation in High-Throughput Experiments** *Bioinformatics* https://doi.org/10.1093/bioinformatics/bts034

Leibowitz S. F., Sladek C., Spencer L., Tempel D. (1988) **Neuropeptide Y, Epinephrine and Norepinephrine in the Paraventricular Nucleus: Stimulation of Feeding and the Release of Corticosterone, Vasopressin and Glucose** *Brain Research Bulletin* **21**:905–12

Likhtik Ekaterina, Johansen Joshua P. (2019) **Neuromodulation in Circuits of Aversive Emotional Learning** *Nature Neuroscience* **22**:1586–97

Love Michael I., Huber Wolfgang, Anders Simon (2014) **Moderated Estimation of Fold Change and Dispersion for RNA-Seq Data with DESeq2** *Genome Biology* **15**

Loy Rebekah, Koziell David A., Lindsey James D., Moore Robert Y. (1980) **Noradrenergic Innervation of the Adult Rat Hippocampal Formation** *The Journal of Comparative Neurology* https://doi.org/10.1002/cne.901890406

Martin Marcel (2011) **Cutadapt Removes Adapter Sequences from High-Throughput Sequencing Reads** *EMBnet.journal* **17**:10–12

Mather Mara, Clewett David, Sakaki Michiko, Harley Carolyn W. (2016) **GANEing Traction: The Broad Applicability of NE Hotspots to Diverse Cognitive and Arousal Phenomena** *The Behavioral and Brain Sciences* **39**

McCall Jordan G., Al-Hasani Ream, Siuda Edward R., Hong Daniel Y., Norris Aaron J., Ford Christopher P., Bruchas Michael R. (2015) **CRH Engagement of the Locus Coeruleus Noradrenergic System Mediates Stress-Induced Anxiety** *Neuron* **87**:605–20

McCall Jordan G., Siuda Edward R., Bhatti Dionnet L., Lawson Lamley A., McElligott Zoe A., Stuber Garret D., Bruchas Michael R. (2017) **Locus Coeruleus to Basolateral Amygdala Noradrenergic Projections Promote Anxiety-like Behavior** *eLife* **6** https://doi.org/10.7554/eLife.18247

McGaugh James L., Roozendaal Benno (2002) **Role of Adrenal Stress Hormones in Forming Lasting Memories in the Brain** *Current Opinion in Neurobiology* **12**:205–10

Meijer Onno C., Buurstede Jacobus C., Viho Eva M. G., Amaya Jorge Miguel, Koning Anne-Sophie C. A. M., van der Meulen Merel, van Weert Lisa T. C. M., Paul Susana N., Kroon Jan, Koorneef Lisa L. (2022) **"Transcriptional Glucocorticoid Effects in the Brain: Finding the Relevant Target Genes."** *Journal of Neuroendocrinology*

Mifsud Karen R., Kennedy Clare L. M., Salatino Silvia, Sharma Eshita, Price Emily M., Haque Samantha N., Gialeli Andriana, et al. (2021) **Distinct Regulation of Hippocampal Neuroplasticity and Ciliary Genes by Corticosteroid Receptors** *Nature Communications* **12**:1–23

Murphy-Royal Ciaran, Johnston April D., Boyce Andrew K. J., Diaz-Castro Blanca, Institoris Adam, Peringod Govind, Zhang Oliver, et al. (2020) **Stress Gates an Astrocytic Energy Reservoir to Impair Synaptic Plasticity** *Nature Communications* **11**

O'Donnell John, Ding Fengfei, Nedergaard Maiken (2015) **Distinct Functional States of Astrocytes during Sleep and Wakefulness: Is Norepinephrine the Master Regulator?** *Current Sleep Medicine Reports* **1**:1–8

Oleskevich S., Descarries L., Lacaille J. C. (1989) **Quantified Distribution of the Noradrenaline Innervation in the Hippocampus of Adult Rat** *The Journal of Neuroscience: The Official Journal of the Society for Neuroscience* **9**:3803–15

Oyarzabal Esteban A., Hsu Li-Ming, Das Manasmita, Chao Tzu-Hao Harry, Zhou Jingheng, Song Sheng, Zhang Weiting, et al. (2022) **Chemogenetic Stimulation of Tonic Locus Coeruleus Activity Strengthens the Default Mode Network** *Science Advances* **8**

Paillasse Michael R., de Medina Philippe (2015) **The NR4A Nuclear Receptors as Potential Targets for Anti-Aging Interventions** *Medical Hypotheses* **84**:135–40

Pan Jie, Ma Nana, Zhong Jie, Yu Bo, Wan Jun, Zhang Wei (2021) **Age-Associated Changes in Microglia and Astrocytes Ameliorate Blood-Brain Barrier Dysfunction** *Molecular Therapy. Nucleic Acids* **26**:970–86

Petit J-M, Eren-Koçak E., Karatas H., Magistretti P., Dalkara T. (2021) **Brain Glycogen Metabolism: A Possible Link between Sleep Disturbances, Headache and Depression** *Sleep Medicine Reviews* **59**

Poe Gina R., Foote Stephen, Eschenko Oxana, Johansen Joshua P., Bouret Sebastien, Jones Gary Aston-, Harley Carolyn W., et al. (2020) **Locus Coeruleus: A New Look at the Blue Spot** *Nature Reviews Neuroscience* https://doi.org/10.1038/s41583-020-0360-9

Popichak Katriana A., Hammond Sean L., Moreno Julie A., Afzali Maryam F., Backos Donald S., Slayden Richard D., Safe Stephen, Tjalkens Ronald B. (2018) **Compensatory Expression of Nur77 and Nurr1 Regulates NF-κB-Dependent Inflammatory Signaling in Astrocytes** *Molecular Pharmacology* **94**:1174–86

Privitera Mattia, Ferrari Kim David, von Ziegler Lukas M., Sturman Oliver, Duss Sian N., Floriou-Servou Amalia, Germain Pierre-Luc, et al. (2020) **A Complete Pupillometry Toolbox for Real-Time Monitoring of Locus Coeruleus Activity in Rodents** *Nature Protocols* **15**:2301–20

Rivas M., Naranjo J. R. (2007) **"Thyroid Hormones, Learning and Memory."** *Genes, Brain, and Behavior* **6**:40–44

Robertson Sabrina D., Plummer Nicholas W., de Marchena Jacqueline, Jensen Patricia (2013) **Developmental Origins of Central Norepinephrine Neuron Diversity** *Nature Neuroscience* **16**:1016–23

Roszkowski Martin, Manuella Francesca, von Ziegler Lukas, Durán-Pacheco Gonzalo, Moreau Jean-Luc, Mansuy Isabelle M., Bohacek Johannes (2016) **Rapid Stress-Induced Transcriptomic Changes in the Brain Depend on Beta-Adrenergic Signaling** *Neuropharmacology* **107**:329–38

Rubin Todd G., Gray Jason D., McEwen Bruce S. (2014) **"Experience and the Ever-Changing Brain: What the Transcriptome Can Reveal."** *BioEssays: News and Reviews in Molecular, Cellular and Developmental Biology* **36**:1072–81

Sara Susan J (2015) **Locus Coeruleus in Time with the Making of Memories** *Current Opinion in Neurobiology* **35**:87–94

Schwabe Lars, Hermans Erno J., Joëls Marian, Roozendaal Benno (2022) **Mechanisms of Memory under Stress** *Neuron* https://doi.org/10.1016/j.neuron.2022.02.020

Smith M. A., Banerjee S., Gold P. W., Glowa J. (1992) **Induction of c-Fos mRNA in Rat Brain by Conditioned and Unconditioned Stressors** *Brain Research* **578**:135–41

Stankiewicz Adrian M., Goscik Joanna, Majewska Alicja, Swiergiel Artur H., Juszczak Grzegorz R. (2015) **The Effect of Acute and Chronic Social Stress on the Hippocampal Transcriptome in Mice** *PloS One* **10**

Strange Bryan A., Witter Menno P., Lein Ed S., Moser Edvard I. (2014) **Functional Organization of the Hippocampal Longitudinal Axis** *Nature Reviews. Neuroscience* **15**:655–69

Sturman Oliver, Germain Pierre-Luc, Bohacek Johannes (2018) **Exploratory Rearing: A Context- and Stress-Sensitive Behavior Recorded in the Open-Field Test** *Stress* **21**:443–52

Sui L., Wang F., Liu F., Wang J., Li B. M. (2006) **Dorsal Hippocampal Administration of Triiodothyronine Enhances Long-Term Memory for Trace Cued and Delay Contextual Fear Conditioning in Rats** *Journal of Neuroendocrinology* **18**:811–19

Tyssowski K. M., DeStefino N. R., Cho J. H., Dunn C. J., Carty C. E., Jones R. D., Chang S. M., et al. (2018) **Different Neuronal Activity Patterns Induce Different Gene Expression Programs** *Neuron* **98** https://doi.org/10.1016/j.neuron.2018.04.001

Uematsu Akira, Tan Bao Zhen, Johansen Joshua P. (2015) **Projection Specificity in Heterogeneous Locus Coeruleus Cell Populations: Implications for Learning and Memory** *Learning & Memory* **22**:444–51

Villain Hélène, Benkahoul Aïcha, Birmes Philippe, Ferry Barbara, Roullet Pascal (2018) **Influence of Early Stress on Memory Reconsolidation: Implications for Post-Traumatic Stress Disorder Treatment** *PloS One* **13**

Wang C., Song D., Fu J., Wen X. (2020) **SIK1 Regulates CRTC2-Mediated Gluconeogenesis Signaling Pathway in Human and Mouse Liver Cells** *Frontiers in Endocrinology* **11** https://doi.org/10.3389/fendo.2020.00580

Xu Liming, Dan Mo, Shao Anliang, Cheng Xiang, Zhang Cuiping, Yokel Robert A., Takemura Taro, Hanagata Nobutaka, Niwa Masami, Watanabe Daisuke (2015) **Silver Nanoparticles Induce Tight Junction Disruption and Astrocyte Neurotoxicity in a Rat Blood-Brain Barrier Primary Triple Coculture Model** *International Journal of Nanomedicine* **10**:6105–18

Zenger Manuel, Burlet-Godinot Sophie, Petit Jean-Marie, Magistretti Pierre J., Vardjan Nina, Zorec Robert (2017) **"Chapter 9 - Noradrenergic System and Memory: The Role of Astrocytes."** *Noradrenergic Signaling and Astroglia* :183–200

Zerbi Valerio, Floriou-Servou Amalia, Markicevic Marija, Vermeiren Yannick, Sturman Oliver, Privitera Mattia, von Ziegler Lukas, et al. (2019) **Rapid Reconfiguration of the Functional Connectome after Chemogenetic Locus Coeruleus Activation** *Neuron* **103**:702–18

Zhu Anqi, Ibrahim Joseph G., Love Michael I. (2018) **Heavy-Tailed Prior Distributions for Sequence Count Data: Removing the Noise and Preserving Large Differences** *Bioinformatics* **35**:2084–92

Zhu Hu, Aryal Dipendra K., Olsen Reid H. J., Urban Daniel J., Swearingen Amanda, Forbes Stacy, Roth Bryan L., Hochgeschwender Ute (2016) **Cre-Dependent DREADD (Designer Receptors Exclusively Activated by Designer Drugs) Mice** *Genesis* **54**:439–46

Ziegler Lukas M. von, Floriou-Servou Amalia, Waag Rebecca, Rebecca R. Das Gupta, Sturman Oliver, Gapp Katharina, Maat Christina A., et al. (2022) **Multiomic Profiling of the Acute Stress Response in the Mouse Hippocampus** *Nature Communications* **13**

## Article and author information


**Mattia Privitera**
Laboratory of Molecular and Behavioral Neuroscience, Institute for Neuroscience, Department of Health Sciences and Technology, ETH Zurich, Switzerland, Neuroscience Center Zurich, ETH Zurich and University of Zurich, Switzerland
ORCID iD: 0000-0002-5660-5901

**Lukas M. von Ziegler**
Laboratory of Molecular and Behavioral Neuroscience, Institute for Neuroscience, Department of Health Sciences and Technology, ETH Zurich, Switzerland, Neuroscience Center Zurich, ETH Zurich and University of Zurich, Switzerland
ORCID iD: 0000-0002-5942-7928

**Amalia Floriou-Servou**
Laboratory of Molecular and Behavioral Neuroscience, Institute for Neuroscience, Department of Health Sciences and Technology, ETH Zurich, Switzerland, Neuroscience Center Zurich, ETH Zurich and University of Zurich, Switzerland
ORCID iD: 0000-0002-5090-4900

**Sian N. Duss**
Laboratory of Molecular and Behavioral Neuroscience, Institute for Neuroscience, Department of Health Sciences and Technology, ETH Zurich, Switzerland, Neuroscience Center Zurich, ETH Zurich and University of Zurich, Switzerland
ORCID iD: 0000-0003-0212-0324

**Runzhong Zhang**
Laboratory of Molecular and Behavioral Neuroscience, Institute for Neuroscience, Department of Health Sciences and Technology, ETH Zurich, Switzerland
ORCID iD: 0000-0001-6144-5546

**Rebecca Waag**
Laboratory of Molecular and Behavioral Neuroscience, Institute for Neuroscience, Department of Health Sciences and Technology, ETH Zurich, Switzerland, Neuroscience Center Zurich, ETH Zurich and University of Zurich, Switzerland
ORCID iD: 0000-0001-5103-2860

**Sebastian Leimbacher**
Laboratory of Molecular and Behavioral Neuroscience, Institute for Neuroscience, Department of Health Sciences and Technology, ETH Zurich, Switzerland

**Oliver Sturman**
Laboratory of Molecular and Behavioral Neuroscience, Institute for Neuroscience, Department of Health Sciences and Technology, ETH Zurich, Switzerland, Neuroscience Center Zurich, ETH Zurich and University of Zurich, Switzerland
ORCID iD: 0000-0001-6859-4800

**Fabienne K. Roessler**
Laboratory of Molecular and Behavioral Neuroscience, Institute for Neuroscience, Department of Health Sciences and Technology, ETH Zurich, Switzerland
ORCID iD: 0000-0001-6594-1504

**Annelies Heylen**
Laboratory of Neurochemistry and Behavior, Experimental Neurobiology Unit, Department of Biomedical Sciences, University of Antwerp, Wilrijk (Antwerp), Belgium
ORCID iD: 0000-0002-2660-8984

**Yannick Vermeiren**
Laboratory of Neurochemistry and Behavior, Experimental Neurobiology Unit, Department of Biomedical Sciences, University of Antwerp, Wilrijk (Antwerp), Belgium, Division of Human Nutrition and Health, Chair Group of Nutritional Biology, Wageningen University & Research (WUR), Wageningen, Netherlands
ORCID iD: 0000-0002-2091-5326

**Debby Van Dam**
Laboratory of Neurochemistry and Behavior, Experimental Neurobiology Unit, Department of Biomedical Sciences, University of Antwerp, Wilrijk (Antwerp), Belgium, Department of Neurology and Alzheimer Center, University of Groningen and University Medical Center Groningen (UMCG), Groningen, Netherlands
ORCID iD: 0000-0003-4739-6076

**Peter P. De Deyn**
Laboratory of Neurochemistry and Behavior, Experimental Neurobiology Unit, Department of Biomedical Sciences, University of Antwerp, Wilrijk (Antwerp), Belgium, Department of Neurology and Alzheimer Center, University of Groningen and University Medical Center Groningen (UMCG), Groningen, Netherlands, Department of Neurology, Memory Clinic of Hospital Network Antwerp (ZNA) Middelheim and Hoge Beuken, Antwerp, Belgium
ORCID iD: 0000-0002-2228-2964

**Pierre-Luc Germain**
Laboratory of Molecular and Behavioral Neuroscience, Institute for Neuroscience, Department of Health Sciences and Technology, ETH Zurich, Switzerland, Neuroscience Center Zurich, ETH Zurich and University of Zurich, Switzerland, Computational Neurogenomics, Institute for Neuroscience, Department of Health Sciences and Technology, ETH Zürich, Zurich, Switzerland, Laboratory of Statistical Bioinformatics, University of Zürich, Switzerland
ORCID iD: 0000-0003-3418-4218

**Johannes Bohacek**
Laboratory of Molecular and Behavioral Neuroscience, Institute for Neuroscience, Department of Health Sciences and Technology, ETH Zurich, Switzerland, Neuroscience Center Zurich, ETH Zurich and University of Zurich, Switzerland
**For correspondence:** johannes.bohacek@hest.ethz.ch
ORCID iD: 0000-0002-8442-653X

## Copyright

## Editors

Reviewing Editor
**Matthew Hill**
University of Calgary, Calgary, Canada

Senior Editor
**Kate Wassum**
University of California, Los Angeles, Los Angeles, United States of America

**Reviewer #2 (Public Review):**

The present manuscript investigates the implication of locus coeruleus-noradrenaline system in the stress-induced transcriptional changes of dorsal and ventral hippocampus, combining pharmacological, chemogenetic, and optogenetic techniques. Authors have revealed that stress-induced release of noradrenaline from locus coeruleus plays a modulatory role in the expression of a large scale of genes in both ventral and dorsal hippocampus through activation of β-adrenoreceptors. Similar transcriptional responses were observed after optogenetic and chemogenetic stimulation of locus coeruleus. Among all the genes analysed, authors identified the most affected ones in response to locus coeruleus-noradrenaline stimulation as being Dio2, Ppp1r3c, Ppp1r3g, Sik1, and Nr4a1. By comparing their transcriptomic data with publicly available datasets, authors revealed that these genes were upregulated upon exposure to different stressors. Additionally, authors found that upregulation of Ppp1r3c, Ppp1r3g, and Dio2 genes following swim stress was sustained from 90 min up to 2-4 hours after stress and that it was predominantly restricted to hippocampal astrocytes, while Sik1 and Nr4a1 genes showed a broader cellular expression and a sharp rise and fall in expression, within 90 min of stress onset.

The paper is well written and provides a useful inventory of dorsal and ventral hippocampal gene expression upregulated by activation of LC-NA system, which can be used as starting point for more functional studies related to the effects of stress-induced physiological and pathological changes. Sex-differences were also explored which represents a strength of the study.

https://doi.org/10.7554/eLife.88559.2.sa0

**Author Response**

The following is the authors' response to the original reviews.

> ***eLife assessment***
>
> *This manuscript provides novel and important findings regarding the impact of noradrenergic signaling from the locus coeruleus on hippocampal gene expression. The locus coeruleus is the sole source of noradrenaline to the hippocampus and many rapid molecular changes induced by stress are regulated by noradrenaline. This manuscript provides a rigorous investigation into hippocampal genes uniquely regulated by noradrenaline in the presence or absence of stress. Data were collected and analyses were performed using solid methodology, and the results mostly convincingly support the conclusion made with few weaknesses. The study would benefit from a more comprehensive analyses of sex differences.*

Response: We thank the reviewers and the editors for the positive evaluation of our work and for the constructive feedback. To address some of the key criticisms, we have performed several new experiments and analyses. Importantly, we now provide a much more rigorous

comparison of males and females, which strongly suggests that there are no major sex differences in the transcriptomic response to stress and noradrenaline in the hippocampus. We think that these - and other additions discussed below - significantly strengthen the manuscript. We provide detailed responses to all the reviewers comments. We have added numbers to the reviewers' comments for easier referencing.

> ***Reviewer #1 (Public Review):***
>
> *Comment 1: Privitera et al., provide a comprehensive and rigorous assessment of how noradrenaline (NA) inputs from the locus coeruleus (LC) to the hippocampus regulate stress-induced acute changes in gene expression. They utilize RNA-sequencing with selective activation/inhibition of LC-NA activity using pharmacological, chemogenetic and optogenetic manipulations to identify a great number of reproducible sets of genes impacted by LC activation. It is noteworthy that this study compares transcriptomic changes in the hippocampus induced by stress alone, as compared with selective circuit activation/inhibition. This reveals a small set of genes that were found to be highly reproducible. Further, the publicly available data will be highly useful to the scientific community.*

Response: We are very grateful for this positive evaluation.

> *Comment 2: A major strength of the study is the inclusion of both males and females. However, with this aspect of the study also lies the biggest weakness. While the experiments tested males and females, they were not powered for identifying sex differences. There are vast amounts of literature documenting the inherent sex differences, both under resting and stress-evoked conditions, in the LC-NA system and this is a major missed opportunity to better understand if there is an impact of these sex-specific differences at the genetic level in a major LC projection region. There are many instances whereby sex effects are apparent, but do not pass multiple testing correction due to low n's. The authors highlight one of them (Ctla2b) in supplemental figure 6. This gene is only upregulated by stress in females. It is appreciated that the manuscript provides an incredible amount of novel data, making the investigation of sex differences ambitious. Data are publicly available for others to conduct follow up work, and therefore it may be useful if a list of those genes that were different based on targeted interrogation of the dataset be provided with a clear statement that multiple testing corrections failed. This will aid further investigations that are powered to evaluate sex effects.*

Response: The assessment of the reviewers and the editorial feedback encouraged us to look more thoroughly into potential sex differences, because we believe it would indeed be a major additional strength if our manuscript could make a firm statement on this important issue. To this end, we have expanded the manuscript in two major ways:

(1) To expand the analysis of sex effects also to the dorsal hippocampus, and to increase robustness of the data, we have performed RNA-seq in 32 additional samples of male and female mice exposed to stress (or control) and propranolol (or saline) injection. Figure 1fh and Supplementary Figure 1d-f have been updated to reflect this new addition, and the results are presented in a new section on Pages 3-4 (pasted below for ease of reviewing). In summary, the strongly support our initial observation that the effects of stress on gene expression, as well as the effects of propranolol on blocking stress-induced effects, are highly similar in both sexes.

(2) To further increase the power for detection of sex-effects, we have performed a small meta-analysis. For this, we combined several RNAseq datasets from the current manuscript and published datasets from our previous work (Floriou-Servou et al., 2018; von Ziegler et al.,

2022), which also investigated transcriptomic sex-differences in the hippocampus 45 min after cold swim stress exposure in the same setup as used for the current manuscript. This approach increased our sample size to 51 males and 20 females. In summary, this well-powered approach shows no evidence for sex differences in the transcriptional response to stress, even when more lenient analyses were applied. These results are described in a new section on page 4, and summarized in Supplementary Figures 1f+g. This section is pasted below for ease of reviewing.

"While blocking β-adrenergic receptors was able to block stress-induced gene expression, we did not test whether propranolol might decrease gene expression already at baseline, independent of stress. Additionally, all tests had thus far been conducted in male mice, raising the question about potential sex differences in NA-mediated transcriptomic responses. To address these two issues, we repeated the experiment in both sexes and included a group that received a propranolol injection but was not exposed to stress (Fig. 1f). Combining the data from both experiments, we repeated the analysis for each region, to identify genes whose response to stress was inhibited by propranolol (Figure 1g). As in the previous experiment, we found that many of the stress-induced gene expression changes were blocked by propranolol injection in both dHC (Figure 1g, left panel) and vHC (Figure 1g, right panel). Importantly, propranolol did not change the expression level of these genes in the absence of stress. We then directly compared the genes sensitive to stress and propranolol treatment in both dHC and vHC. To this end, we plotted the union of genes showing a significant stress:propranolol interaction in either region in one heatmap across both dHC and vHC (Supplementary Figure 1d). This showed again that the stress-induced changes were very similar in dHC and vHC, and that propranolol similarly blocked many of them. Finally, we asked whether the response differs between males and females. Despite clear sex differences in gene expression at baseline (data not shown), we found no significant sex differences in response to stress or propranolol between male and female mice (FDR<0.05; Fig. 1g). To more directly visualize this, we compared females and males by plotting the log2-fold changes of the stress:propranolol interaction across all stress-induced genes that were blocked by propranolol. We find very similar regulation patterns in both sexes (Figure 1h). Although none of these sex differences are significant, some genes seem to show quantitative differences, so we plotted the expression patterns of the 5 genes showing the largest difference in interaction term as box-plots, which suggest that these spurious differences are likely due to noisy coefficient estimates (Supplementary Fig. 1e). To address concerns that our analysis of sex differences might not have been sufficiently powered, we performed a meta-analysis of the experiments shown here along with previously published datasets from our lab (Floriou-Servou et al. 2018; von Ziegler et al. 2022). In all these experiments, the vHC of male and female mice was profiled 45 min after exposure to an acute swim stress challenge. This resulted in a sample size of 51 males and 20 females. Despite this high number of independent samples, we could not identify any statistically significant interaction between sex and the stress response. To identify candidates that might not reach significance while discounting differences due to noise in fold-change estimates, we reproduced the same analysis using DESeq2 with Approximate Posterior Estimation for generalized linear model (apeglm) logFC shrinkage (A. Zhu, Ibrahim, and Love 2018). This analysis also did not reveal any sex differences in the stress response (Supplementary Fig. 1f). We then tailored the meta-analysis specifically to the set of stress-responsive genes that were blocked by propranolol, and also for these genes the response to stress was strikingly similar in both sexes (Supplementary Fig. 1g). Altogether, we conclude that there are no major sex differences in the rapid transcriptomic stress response in the hippocampus, and that blocking beta-receptors prevents a large set of stress-induced genes in both females and males."

To put these findings in context with existing literature, we agree with the reviewer that there are many studies that have reported sex differences in the LC-circuitry as summarized by Bangasser and colleagues (Bangasser et al., 2016, 2019). However, these studies primarily focus on the LC itself, suggesting that female rats have more LC neurons, denser LC-dendrites

in the peri-LC region, and that LC neurons are more readily activated by stress in females because of heightened sensitivity to CRF-signaling. A recent study in mice reports, in contrast, that females have fewer TH-positive neurons in the LC, but they also find enhanced excitability of LC neurons in females (Mariscal et al., 2023). Similarly, one study has suggested molecular differences in the makeup of the LC (Mulvey et al., 2018). Our experiments, however, focus on the impact of NA release in a projection region (hippocampus). Further, we use a strong stress induction protocol (swim stress) and various potent modes of direct LC activation, so differences in "LC-excitability" are likely less relevant in this context. We added evidence showing that we trigger powerful NA release in both sexes (Supplementary Figure 2c-h; see response to Reviewer #2, Comment #3 for more details). In addition, we show that the intensity or pattern of LC stimulation does not appear to alter the molecular response (Figure 3a-b), and that various stressors (mild or intense) all trigger the same NA-dependent molecular changes (Figure 4a-b). Therefore, our results suggest that once NA is released (in the hippocampus), the molecular downstream effects on gene expression are very similar - independent of stimulation intensity, sex, or hippocampal subregion (dorsal/ventral). This does not mean that there are no sex differences for activation of LC, but rather that the transcriptional response to NA release in the hippocampus is robust across sexes, and that propranolol seems to block NA-dependent effects similarly in both sexes. This does not rule out quantitative differences between sexes that only emerge with targeted analyses of individual genes, or once fluctuations in ovarian hormones are taken into account. We have updated the section in the discussion to summarize these considerations in light of the new results (see pages 20-21, section: "A uniform molecular response to stress and noradrenaline release in both sexes").

> *Comment 3: A major finding of the present study is the involvement of noradrenergic transcriptomic changes occurring in astrocytic genes in the hippocampus. Given the stated importance of this finding within the discussion, it seems that some additional dialogue integrating this with current literature about the role of astrocytes in the hippocampus during stress or fear memory would be important.*

Response: We thank the reviewer for giving us an opportunity to add a more detailed discussion about the role of astrocytes and thyroid hormones in the hippocampus during learning and memory formation. We have added these statements to the discussion:

“Within the hippocampus, astrocytic pathways are emerging as important players for learning and memory processes (Gibbs, Hutchinson, and Hertz 2008; Bohmbach et al. 2022). In fact, it is well-known that NA enhances memory consolidation (Schwabe et al. 2022; McGaugh and Roozendaal 2002), and recent work suggests that these effects are mediated by astrocytic β-adrenergic receptors (Gao et al. 2016; Iqbal et al. 2023). Our transcriptomic screens revealed Dio2 as the most prominent target influenced by LC activity. Dio2 is selectively expressed in astrocytes and encodes for the intracellular type II iodothyronine deiodinase, which converts thyroxine (T4) to the bioactive thyroid hormone 3,3',5-triiodothyronine (T3) and therefore regulates the local availability of T3 in the brain (Bianco et al. 2019). Enzymatic activity of DIO2 has further been shown to be increased by prolonged noradrenergic transmission through desipramine treatment in LC projection areas (Campos-Barros et al. 1994). This suggests that the LC-NA system and its widespread projections could act as a major regulator of brain-derived T3. Notably, T3-signaling plays a role in hippocampal memory formation (Rivas and Naranjo 2007; Sui et al. 2006), raising the possibility that NA-induced Dio2 activity in astrocytes might mediate some of these effects.”

> *Comment 4: The comparison of the candidate genes activated by the LC in the present study (swim) with datasets published by Floriou-Servou et al., 2018 (Novelty, swim, restraint, and footshock) is an interesting and important comparison. Were there other stressors identified in this paper or other publications that do not regulate these*

> *candidate genes? Further, can references be added to clarify to the reader, that prior studies have identified that novelty, restraint and footshock all activate LC-NA neurons.*

ponse: Thank you for the positive feedback. We have only tested the stressors reported in Figure 4a-b (novelty, swim, restraint, and footshock). It is known that all these stressors trigger noradrenaline release, in fact we are not aware of stressors that do not trigger NA release. This reproducible finding supports the notion that the identified set of genes is indeed highly NAresponsive. As suggested, we have now included references that show increased NA release in response to all these stressors:

“Therefore, we assessed their expression in a dataset comparing the effect of various stressors on the hippocampal transcriptome (Floriou-Servou et al., 2018). The stressors included restraint, novelty and footshock stress, which have all previously been shown to increase hippocampal NA release (HajósKorcsok et al., 2003; Lima et al., 2019; Masatoshi Tanaka et al., 1982).”

> *Comment 5: Comparisons are made between chemogenetic studies and yohimbine, stating that fewer genes were activated by chemogenetic activation of LC neurons. There is clear justification for why this may occur, but a caveat may need to be mentioned, that evidence of neuronal activation in the LC by each of these methods were conducted at 90 (yohimbine) versus 45 (hM3Dq) minutes, and therefore it cannot be ruled out that differences in LC-NA activity levels might also contribute.*

Response: The reviewer raises an important point about some inconsistencies between the time points chosen in our study, an aspect that was also pointed out by Reviewer #2. We have chosen the 45 and 90 min time points for two different reasons. On the one hand, cFos changes on the protein level are known to peak 90 min after neuronal activation, and we wanted to capture the strongest possible cFos signal in the LC. On the other hand, we wanted to measure gene expression changes triggered by NA release, which already occur 45 min after noradrenergic activation (Roszkowski et al., 2016). Thus, when the experimental design allowed separate experiments (e.g. systemic yohimbine injection), we chose to measure gene expression after 45 min, but to validate cFos activation in the LC separately after 90min. In response to DREADD activation, however, we wanted to confirm within the same animal that LC activation was successful, and thus we collected LC and hippocampus simultaneously (Figure 2c,d). While the cFos increase is already very pronounced at the 45min time point (Figure 2g), the quality of IHC is slightly lower because the tissue cannot be perfused in this experimental design. Therefore, we do not think that the time point for cFos sampling matters in this context. However, we agree with the reviewer that it remains unclear whether yohimbine and DREADDs activate the LC with similar potency. To directly compare NA release would require a set of photometry-based experiments to measure NA release using genetically-encoded NA-sensors. While we have added such experiments for LC activation with DREADDs and optogenetics to show rapid NA release indeed occurs in the hippocampus (see Reviewer #2, Comment 3; Supplementary Figure 2c-h), yohimbine interferes with the NA-sensors as explained in detail in response to Reviewer 2, Comment 3. Thus, it was too challenging for us to directly compare the release dynamics in response to DREADDs and yohimbine, which was also not the main focus of our work. To explicitly address this caveat, we have extended the corresponding section in the discussion:

"Finally, our observation that systemic administration of the α2-adrenergic receptor antagonist yohimbine very closely recapitulates the transcriptional response to stress stands in contrast to the much more selective transcriptional changes observed after chemogenetic or optogenetic LC-NA activation. This difference could be due to various factors. First, it remains unclear how strong the LC gets activated by yohimbine versus hM3Dq-DREADDs. However, given the potent LC activation observed after DREADD activation, it seems unlikely that yohimbine would lead to a more pronounced LC activation, thus explaining the stronger

transcriptional effects. Second, contrary to LC-specific DREADD-activation, systemic yohimbine injection will also antagonize postsynaptic α2-adrenergic receptors throughout the brain (and periphery). More research is needed to determine whether this could have a more widespread impact on the hippocampus (and other brain regions) than isolated LC-NA activation, further enhancing excitability by preventing α2-mediated inhibition of cAMP production. Finally, systemic yohimbine administration and noradrenergic activity have been shown to induce corticosterone release into the blood (Johnston, Baldwin, and File 1988; Leibowitz et al. 1988; Fink 2016). Thus, yohimbine injection could have broader transcriptional consequences, including corticosteroid-mediated effects on gene expression."

> *Comment 6: Please add information about how virus or cannula placement was confirmed in these studies. Were missed placements also analyzed separately?*

Response: Pupillometry recordings were performed with all animals involving optogenetic or chemogenetic manipulations of the LC, before subjecting them to stress experiments. These assessments account for both correct optic fiber placement and virus expression (Privitera et al., 2020). If an animal did not show a clear pupil response, it was not included any further in the study. To demonstrate correct cannula placement for drug infusion of isoprotenerol in the dorsal hippocampus, we added a representative image of cannula placement in Supplementary Figure 1h.

> *Comment 7: Time of day for tissue collection used in genetic analysis should be reported for all studies conducted or reanalyzed.*

Response: Thank you for pointing out this omission. Tissue collection for RNA-seq analysis was always performed between 11am and 5pm during the dark phase of the reversed light-dark cycle. We have added this information to the corresponding method section ("Tissue collection").

> ***Reviewer #1 (Recommendations For The Authors):***
>
> *Comment 8: This is a well written, comprehensive and rigorous manuscript that will be of great interest to those in the scientific community.*

Response: Thank you for the positive evaluation of our work and for the constructive feedback.

> ***Reviewer #2 (Public Review):***
>
> *Comment 1: The present manuscript investigates the implication of locus coeruleus-noradrenaline system in the stress-induced transcriptional changes of dorsal and ventral hippocampus, combining pharmacological, chemogenetic, and optogenetic techniques. Authors have revealed that stress-induced release of noradrenaline from locus coeruleus plays a modulatory role in the expression of a large scale of genes in both ventral and dorsal hippocampus through activation of β-adrenoreceptors. Similar transcriptional responses were observed after optogenetic and chemogenetic stimulation of locus coeruleus. Among all the genes analysed, authors identified the most affected ones in response to locus coeruleus-noradrenaline stimulation as being Dio2, Ppp1r3c, Ppp1r3g, Sik1, and Nr4a1. By comparing their transcriptomic data with publicly available datasets, authors revealed that these genes were upregulated upon exposure to different stressors. Additionally, authors found that upregulation of Ppp1r3c, Ppp1r3g, and Dio2 genes following swim stress was sustained from 90 min up to 2-4 hours after stress and that it was predominantly restricted to hippocampal astrocytes, while Sik1 and Nr4a1 genes showed a broader cellular expression and a sharp rise and fall in expression, within 90 min of stress onset.*

> *Overall, the paper is well written and provides a useful inventory of dorsal and ventral hippocampal gene expression upregulated by activation of LC-NA system, which can be used as starting point for more functional studies related to the effects of stress-induced physiological and pathological changes.*

Response: We thank the reviewer for the careful assessment of our work.

> *Comment 2: However, I believe that the study would have benefited of a more comprehensive analyses of sex differences. Experiments in females were conducted only in one experiment and analyses restricted to the ventral hippocampus.*

Response: In response to the comments by the reviewer, as well as Reviewer #1 and the editors, we have sequenced an additional 32 brain samples to expand the comparison of sex effects in females and males across dorsal and ventral hippocampus, and we included a new meta-analysis of 3 experimental datasets (51 male and 20 female) samples, to thoroughly assess sex differences in the transcriptomic response to stress. We refer the reviewer to our detailed response provided above to Reviewer #1, comment #2, and the updated results section on pages 3-4.

> *Comment 3: Although, the experiments were overall sound and the results broadly support the conclusion made, I think some methodological choices should be better explained and rationalized. For instance, the study focuses on identifying transcriptional changes in the hippocampus induced by stress-mediated activation of the LC-NA system, however NA release following stress exposure and pharmacological or optogenetic manipulation was mostly measured in the cortex.*

Response: Because the hippocampus was used for RNA-sequencing, we could not assess NA release in the hippocampus (as this would require fiber implants that would interfere with molecular measures, or different tissue processing for HPLC). Nonetheless, we wanted to assess the transcriptional changes in the hippocampus, while simultaneously measuring successful stimulation of the LC-NA system in the same animals. To achieve this, we pursued 3 routes: 1) we used pupillometry to confirm functional LC activation; 2) we measured cFOS in the LC to directly demonstrate LC activation; 3) we assessed NA release using uHPLC (which requires larger tissue samples) and we chose the cortex because both cortex and hippocampus receive NA predominantly from the LC (Samuels & Szabadi, 2008). Importantly, we had previously shown that chemogenetic LC activation leads to a similar NA turnover in both the cortex and hippocampus, as measured by uHPLC (Zerbi et al., 2019). The relevant figure from that paper is inserted below to quickly show the striking similarity between hippocampus and cortex.

**Author response image 1.**

Levels of noradrenaline (NE) turnover (MHPG/NE ratio) in the cortex (CTX) and hippocampus (HC), measured in whole tissue with uHPLC 90min after hM3Dq-DREADD activation of the LC (copied and cropped from Zerbi et al, 2019, Neuron).

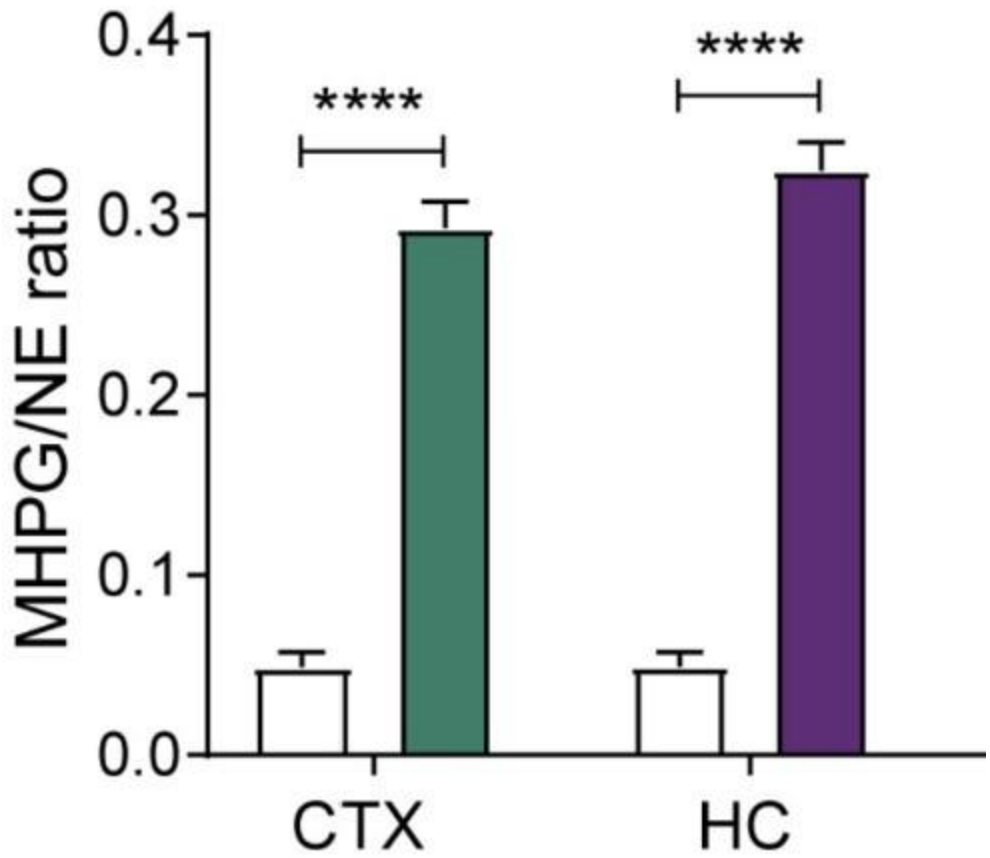


In response to the reviewers comment, we performed additional experiments to directly demonstrate that LC-activation with DREADDs as well as optogenetics causes an increase in hippocampal NA-release. We recorded NA release in the hippocampus (using fiber photometry combined with genetically encoded NA sensors). For DREADD activation, we observed a strong increase in hippocampal noradrenaline that started a few minutes after clozapine administration, and this increase was sustained throughout the duration of the 21 minute recording (see Supplementary Figure2c-e). For optogenetic LC activation, we find a rapid and immediate sharp increase in NA levels in the hippocampus (Supplementary Figure 2f-h). These experiments were performed in females and males and triggered similar responses. An adapted and cropped version of Supplementary Figure 2 is pasted below for ease of reading.

Please note that we could not perform a similar experiment using yohimbine, because the GRABNE sensors are based on the alpha-2 adrenergic receptor, thus yohimbine administration interferes with the photometry recording. However, we believe that it is clear from this response that strong activation of the LC leads to uniform release of NA in the hippocampus and cortex.

**Author response image 2.**

c, Schematic of fiber photometry recording of hippocampal NA during chemogenetic activation of the LC. After 5 min baseline recording in the homecage animals were injected with clozapine (0.03mg/kg, i.p.) and placed in the OFT for 21min. d, Average ΔF/F traces of GRABNE2m photometry recordings in response to chemogenetic activation of the LC (mean±SEM for hM3DGq+ and hM3DGq- split into females and males, n=3/group/sex). e, Peak ΔF/F response of fiber photometry trace. f, Schematic of fiber photometry recording of

hippocampal NA during optogenetic activation of the LC. Animals were lightly anesthetized (1.5% isoflurane) and recorded in a stereotaxic frame. After 1 min baseline recording, animals were stimulated three times with 5Hz for 10s (10ms pulse width, ~8mW laser power) and recorded for 2 min post-stimulation. g, Average ΔF/F traces of the NA sensors GRABNE1m and nLightG in response to optogenetic activation of the LC (mean±SEM for females and males, n(females)= 10, n(males)=5. h, Peak ΔF/F response of fiber photometry trace.

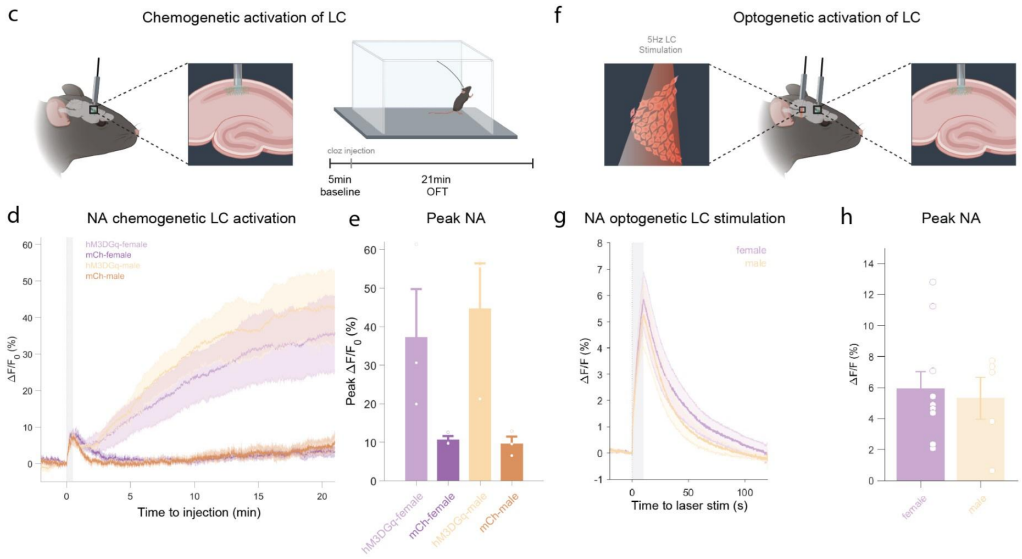


> *Comment 4: Furthermore, behavioral changes following systemic pharmacologic or chemogenetic manipulation were observed in the open field task immediately after peripheral injections of yohimbine or CNO, respectively. Is this timing sufficient for both drugs to cross the blood brain barrier and to exert behavioral effects?*

Response: We have previously shown that chemogenetic activation of the LC through clozapine elicits pupil responses within 1-2 minutes after injection (Privitera et al., 2020; Zerbi et al., 2019). This indicates that clozapine rapidly crosses the blood brain barrier and affects LC activity within a few minutes after injection. Our additional experiments using genetically encoded sensors in the hippocampus show this even more directly (Supplementary Figure 2d), see also the response to Comment 3 above.

Similarly, yohimbine also rapidly crosses the blood brain barrier within the same time frame (Hubbard et al., 1988). These observations are consistent with the rapid behavioral effects that can be detected within a few minutes after injection of clozapine for LC-DREADD activation (Zerbi et al., 2019), and for yohimbine as well (von Ziegler et al., 2023). In response to another comment of this reviewer, we have also re-analyzed the behavior presented in the current manuscript in time-bins of 3 minutes, which also shows the rapid onset of effects in response to yohimbine (within the first 3 min) and DREADDs (within 6 min), see Supplementary Fig. 3.

> *Comment 5: Finally, the study shows that activation of noradrenergic hippocampus-projecting LC neurons is sufficient to regulate the expression of several hippocampal genes, although the necessity of these projection to induce the observed transcriptional effects has been tested to some extent through systemic blockade of beta-adrenoceptor, I believe the study would have benefited of more selective (optogenetic or chemogenetic) necessity experiments.*

Response: We understand the reviewer's point that blocking the LC during stress exposure would be an interesting experiment. However, it is very hard to completely silence the LC during intense stressors. In fact, despite intense efforts, we have not been able to silence the LC during swim stress exposure using DREADDs or other chemogenetic approaches (PSAM/PSEM). We were in fact able to silence the LC with the optogenetic inhibitor JAWS (and others have reported successful LC silencing with GtACR2), but there is a major issue involving the "rebound effect", where more NA is released once the inhibition is stopped. We would thus have had to optogenetically silence the LC for 45-90 min, which would create heat artifacts, and require challenging control experiments to draw firm conclusions. Given all these issues, we reasoned that blocking adrenergic receptors is a simple and elegant solution, which provides clear evidence for the necessity of beta-adrenergic signaling.

> ***Reviewer #2 (Recommendations For The Authors):***
>
> *Major concerns:*
>
> *Comment 6: The study focuses on the identification of transcriptional changes in the hippocampus induced by stress-mediated activation of the LC-NA system, however, noradrenaline release following stress exposure or yohimbine injection was measured in the cortex. Authors should consider measuring NA concentrations in the hippocampus after exposure to swim stress or administration of yohimbine, or at least explain their choice to analyse to cortex in the manuscript.*

Response: We have addressed this issue in detail in Response to "Reviewer 2, Comment #3", where we provided an overview of the additional data that support our approach. As mentioned before, measuring NA release after yohimbine is not compatible with our GRABNE-photometry approach, as the GRAB-sensor is based on alpha2-adrenoceptor. Here, we would like to add that measuring NA release using photometry during swim stress is also challenging. The challenge is the vigorous movement (swimming, typically in one direction), which creates pressure on the cables/implants. We felt that overcoming these experimental challenges (setup, troubleshooting and controls) would be beyond the scope of the paper, given that it is already known that this stressor leads to strong NA release in the hippocampus. We have now included references that demonstrate that all the stressors used in our work trigger NA increase in the hippocampus (see response to Reviewer 1, Comment 3): “Therefore, we assessed their expression in a dataset comparing the effect of various stressors on the hippocampal transcriptome (Floriou-Servou et al., 2018). The stressors included restraint, novelty and footshock stress, which have all previously been shown to increase hippocampal NA release (Hajós-Korcsok et al., 2003; Lima et al., 2019; Masatoshi Tanaka et al., 1982).”

> *Comment 7: Concerning the experiment aimed at investigating sex differences in gene expression, it is not clear the reason why authors decided to restrict their analyses in females to the ventral hippocampal only. The explanation that in males they did not detect major differences between the dorsal and ventral hippocampus is not sufficient, because there could have been different effects in females. Therefore, the conclusion made by the authors that their "results suggest that the transcriptomic response is independent of sex" is not entirely correct, since sex differences were only evaluated in the ventral hippocampus.*

Response: We appreciate the reviewer's critique. As described above, we have now also sequenced the dorsal hippocampal tissue from the propranolol experiment (males and females, 32 samples) and additionally added an extensive meta-analysis of three large datasets (n=71) to compare transcriptional sex differences in response to stress. A detailed

description of these experiments and how they have extended/supported our conclusions have been provided in response to Reviewer #1, Comment #2.

> *Comment 8: Besides the effects on females, the same experiment examined whether propranolol by itself (in the absence of stress) would have been able to alter gene expression: such effects were not examined in the dorsal hippocampus. In contrast, in a different experiment, the effects of isoproterenol on genes expression were restricted to the dorsal hippocampus only. Furthermore, related to this latter experiment, intra-dorsal hippocampal injection of isoproterenol should presumably mimic the rise in NA observed after stress exposure, why was gene expression measured 90 min after isoproterenol central injections while in the other experiments gene expression was determined 45 min after stress, that is when authors observe the peak NA concentration?*

Response: We have addressed the reviewer's critique of dorsal vs ventral hippocampus by reanalyzing 32 additional samples from dorsal hippocampus of male and female mice after propranolol (or saline) injection. Please see response to Reviewer #1, comment #2.

Regarding the time points: We have chosen the 45 and 90 min time points mainly for two reasons. First, cFos protein changes are known to be strongest 90 min after neuronal activation. Second, because we wanted to capture gene expression changes triggered by NA release, we reasoned that these effects must be fast and should thus be measured at an early transcriptional time-point (45min). However, after performing the time-course experiment after swim stress exposure (Figure 4d,c), we observed that the LC-NA-sensitive genes (e.g. Dio2 and several PP1-subunits) show the strongest changes 90 min after stress exposure. Therefore, in some of our experiments we opted to analyze gene expression changes at 90min, converging with the time-point we typically use for cFos staining. Contrary to the reviewer's statement, peak NA concentrations are not observed 45 min after the various interventions, but rather the peak in the main metabolite (MHPG) is observed then, due to the temporal dynamics of NA release and breakdown. NA release occurs immediately upon stress exposure (or direct LC activation), which we also show in the new photometry data described above. Thus, rapid NA release triggers intracellular cascades that lead to downstream transcriptional changes, which peak presumably between 4590 min later.

> *Comment 9: Behavioral changes following systemic pharmacologic or chemogenetic manipulation were observed in the open field task immediately after peripheral injections of yohimbine or CNO, respectively. Is this timing sufficient for both drugs to cross the blood brain barrier and to exert behavioral effects? It is also not immediately clear the reason why the open field tasks have different durations depending on the experiments, which can also impact the results. Authors might also consider to split the open field data analyses in 2 or 3 min time-bins, to allow for a better comparison across the different results.*

Response: We thank the reviewer for the suggestion to plot the behavior data as time-bins. We have implemented this change for the yohimbine and DREADD experiments, and updated the corresponding figure accordingly (Supplementary Figure 3, pasted below for ease of reading). The new visualization clearly shows that yohimbine injection triggers rapid behavioral effects already in the first three minutes, whereas the LC-DREADD activation triggers behavioral changes within 3-6 minutes after injection. Thus, clear drug effects are visible in the first 10 minutes, which is comparable to the standard OFT test (10min testing) shown in response to swim stress exposure (Suppl. Figure 3a). The choice to expose mice to the OFT for 21 minutes in total was due to the fact that we based our experimental approach on the optogenetic LC-stimulation protocol first published by McCall and colleagues (McCall et al, Neuron, 2015), in which the LC is stimulated for 3 min followed by 3 min pauses (see Suppl. Figure 3d). Because of this on-off design, we decided to keep the optogenetic analysis

simple and show the overall effect (Supplementary Figure 3d), particularly as we know that NA dynamics do not recover rapidly enough after 3 min continuous stimulation to justify a bin-analysis (unpublished data).

**Author response image 3.**

Effects of acute stress and noradrenergic stimulation on anxiety-like behaviour in the open field test. a, Stress-induced changes in the open field test 45 min after stress onset. Stressed animals show overall reductions in distance traveled (unpaired t-test; t=3.55, df=22, p=0.0018), time in center (welch unpaired t-test; t=3.50, df=13.61, p=0.0036), supported rears (unpaired t-test; t=3.39, df=22, p=0.0026) and unsupported rears (unpaired t-test; t=5.53, df=22, p = 1.47e-05) compared to controls (Control n = 12; Stress n = 12). This data have been previously published (von Ziegler et al., 2022). b, Yohimbine (3 mg/kg, i.p.) injected animals show reduced distance traveled (unpaired t-test; t=2.39, df=10, p=0.03772), reduced supported rears (unpaired t-test; t=6.56, df=10, p=0.00006) and reduced unsupported rears (welch unpaired t-test; t=3.69, df=4.4, p = 0.01785) compared to vehicle injected animals (Vehicle n = 6; Yohimbine n = 7). c, Chemogenetic LC activation induced changes in the open field test immediately after clozapine (0.03 mg/kg, i.p.) injection. hM3Dq+ animals show reduced distance traveled (unpaired t-test; t=6.28, df=13, p=0.00003), reduced supported rears (unpaired t-test; t=4.28, df=13, p=0.0009), as well as reduced unsupported rears (welch unpaired t-test; t=4.28, df=13, p = 0.00437) compared to hM3D- animals (hM3Dq- n = 7; hM3Dq+ n = 8). d, Optogenetic 5 Hz LC activation induced changes during the open field test. ChR2+ animals show reduced supported rears (unpaired t-test; t=2.42, df=64, p=0.0185) and reduced unsupported rears (unpaired ttest; t=2.91, df=64, p = 0.00499) compared to ChR2- animals (ChR2- n = 32; ChR2+ n = 36). Data expressed as mean ± SEM. *p < 0.05, **p < 0.01, ***p < 0.001, ****p < 0.0001.

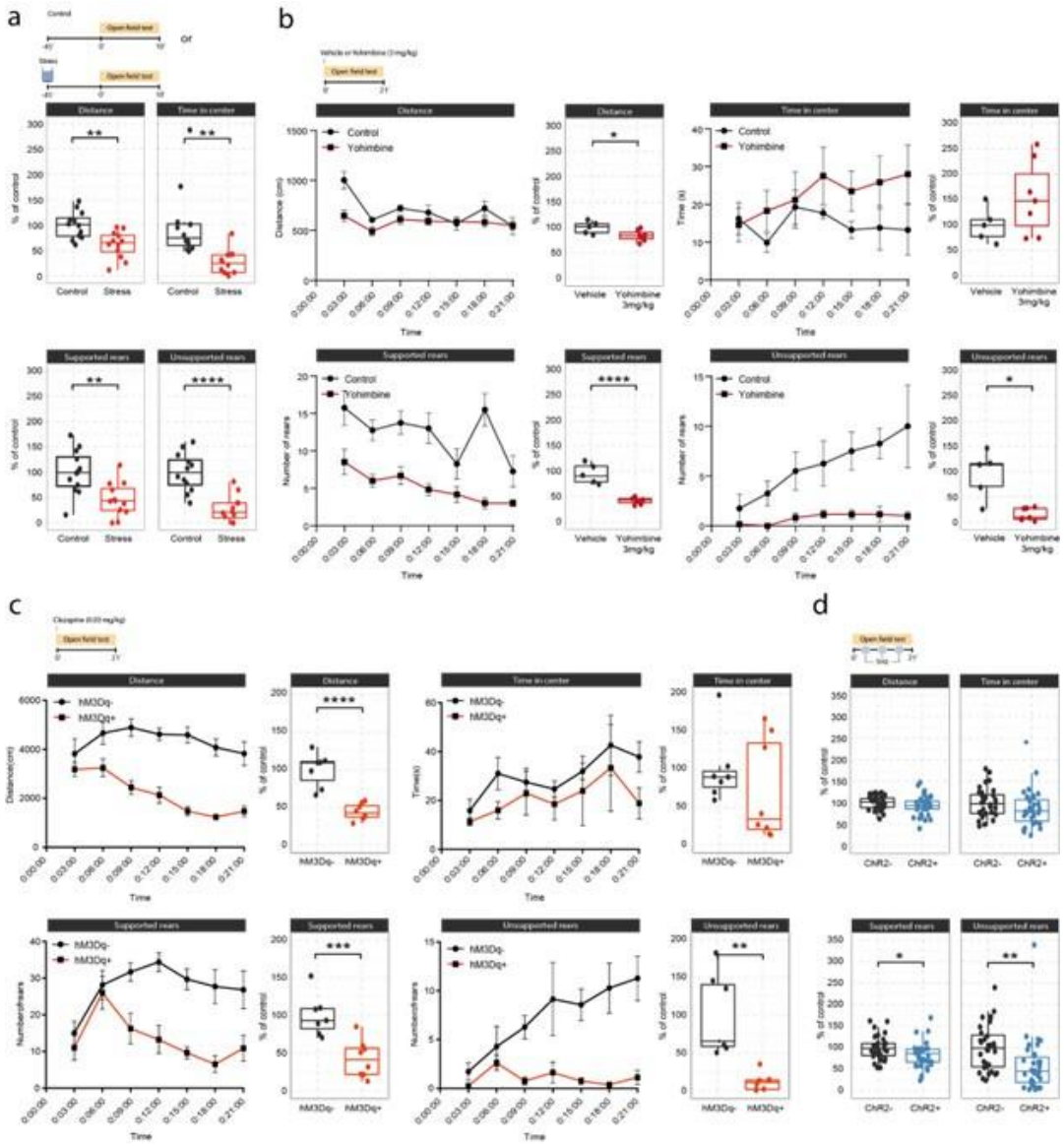


> *Comment 9: The study shows that activation of noradrenergic hippocampus-projecting LC neurons is sufficient to regulate the expression of several hippocampal genes. I believe the study would have benefited of more selective necessity experiments. Authors might consider adding optogenetic (or chemogenetic) experiments aimed at inhibiting LC-NA hippocampal projections during stress exposure (or, alternatively, perform intrahippocampal pharmacological blockade of β-adrenoreceptors during stress exposure), and determine the effects on gene expression.*

Response: We kindly refer the reviewer to our previous response to Comment #2 above.

> *Minor concerns:*
>
> *There is a typo in the abstract. Please correct "LN-NA" with "LC-NA"*

Response: Thank you, we have corrected it.

References

Bangasser, D. A., Eck, S. R., & Ordoñes Sanchez, E. (1/2019). Sex differences in stress reactivity in arousal and attention systems. Neuropsychopharmacology: Official Publication of the American College of Neuropsychopharmacology, 44(1), 129–139.

Bangasser, D. A., Wiersielis, K. R., & Khantsis, S. (06/2016). Sex differences in the locus coeruleusnorepinephrine system and its regulation by stress. Brain Research, 1641, 177–188.